Declaration of Authorship

I, Shine-Od Mongoljiibuu, hereby confirm that I have written the accompanying thesis myself, without contributions from sources other than those cited in the text and acknowledgements.

This also applies to all figures, drawings, maps, and images included in the thesis.

Freiberg, 13.04.2022 _____

Shine-Od Mongoljiibuu

Acknowledgement

This thesis work was done with the contribution of the following:

To Helmholtz Institute Freiberg for Resources and Technology (HZDR/HIF) for allowing me to write this thesis;

To Prof Carsten Drebenstedt and Dr Nils Hoth for the support throughout my study and thesis work;

To my supervisor Dr Norman Kelly for the unconditional patient guidance, encouragement, support in all experimental work, and advice on the thesis writing;

To Dr Martin Rudolph, Dr Robert Möckel, Dr Bradley Guy, Edgar Schach, Doreen Ebert, Stefanie Schubert, Maja Klöden, and Kevin Richter for helping me with my samples, experimental works, analyses, and technical support;

To Advanced Mineral Resources Development (AMRD) program classmates for the help and friendship;

To the family for the unconditional support.

List of Figures

List of Tables

List of abbreviations

AFK	Processing of fine-grained polymetallic native Sn/W/In complex ores
ANOVA	Analysis of Variance
GXMAP	MLA grain-based X-ray mapping
ICP-OES	Inductively Coupled Plasma-Optical Emission Spectroscopy
IRR	Internal Rate of Return
LDS	Laser Diffraction Sensor
NPV	Net Present Value
PSD	Particle size distribution
RLE	Roasting-Leaching-Electrolysis
rpm	rotation per minute
S/L	Solid-liquid ratio
SEM	Scanning Electron Microscope
XRD	X-ray Diffraction
XRF	X-ray Fluorescence

Table of contents

1 Introduction

The demand for raw materials and metals has increased as the world population with high prosperity grows, and technologies are modernizing (Hilgers & Becker, 2020). Moreover, another good reason for increasing demand is energy- and mobility transition, which require a wide variety of raw materials. Additionally, there always have been several issues with the production of raw materials, such as negative impacts on the environment, mining waste, land occupation, and, most importantly, human health issues. Therefore, more sustainable approaches are essential to reduce major environmental problems and risks, such as greenhouse gas reduction and many human health problems.

Around 13.2 million metric tons of refined zinc were consumed globally in 2020 (• *Zinc Metal* Consumption 2020 | Statista, n.d.). Zinc is the most used non-ferrous metal, after aluminium and copper, and is attractive due to its high recyclability. It is found in various applications as a form of metal and its compounds in our daily lives. Applications of zinc are, namely, a protective coating for steel and iron because of its corrosion resistance. Another application is zinc alloy that forms parts of automobile vehicles, rubber, ceramics, and paints. 70% of zinc is mainly produced from sphalerite worldwide.

Sphalerite is also an essential source of several other metals such as cadmium, gallium, germanium, and indium. Frenzel et al. (2017) concluded that 76% of all indium-containing zinc sulphide concentrates is already extractable. Indium is usually used to produce indium tin oxide, a vital part of touch screens, flatscreen TVs, and solar panels due to its electrical conductivity and strong glass bond. Furthermore, indium alloy has been used for fire sprinkler systems because of its low melting point. The demand of indium for small LCD panels for smartphones, tablets, and e-books is likely to expand, whereas growth rates for large-size panels are expected to be low (Ylä-Mella & Pongrácz, 2016).

Moreover, the European Commission and the US Department of Energy have classified indium as a critical material due to its future supply. Previous studies concluded that geological scarcity would not be an issue in the short to mid-term. However, the problem arises due to its dependency on mining its carrier metal, zinc. About 80% of the primary production of indium is in China, South Korea, and Japan. Such a geographical concentration of production is typical for critical materials and increases the risk of supply disruptions and volatility of prices due to political and economic reasons.

The processing of complex ores has been developing considering the metal extraction cost, environment, and high recovery rate. Utilization of low-grade ores, rigid raw materials, lower energy consumption, tailings, water management, and the need to use less harmful chemicals are significant challenges concerning future metals production. For a century, the most common processes to extract zinc involved roasting, sintering, or smelting techniques. The

capital and operational costs, dust collection, and acid production are incredibly high. Furthermore, sulphur dioxide, which has harmful adverse effects on the environment, is formed due to the roasting process.

Consequently, there is a need for the study to be carried out for two primary reasons on an industrial scale. Firstly, it is no longer acceptable to set sulphur dioxide waste gases from smelters into the atmosphere. Therefore, technologies such as hydrometallurgy are comparably safer because it produces elemental sulphur instead of sulphur dioxide. Secondly, the present technology cannot reach satisfaction for refining highly disseminated complex ores. Hence, hydrometallurgy is suitable for further studies due to its benefit of processing complex and low-grade ores.

1.1 Motivation/Background of the work

1.1.1 The Tellerhäuser deposit

The polymetallic Zn-Fe-Sn-Cu-In Tellerhäuser skarn ore, was discovered in 1968, is in the western Erzgebirge and has the largest unexploited occurrences of tin (Sn) and indium (In) in Europe.

The Tellerhäuser deposits include various orientations of mineralisation, stratiform deposits, deposits containing veinlets, and alteration zones (Schuppan et al., 2012). They contain cassiterite, the most valuable mineral, and magnetite and sulphides. Thus, these polymetallic skarn ores require a complex challenge for mineral processing.

The mineralogy of the skarns is very complex and shows considerable variability essential to replacement reactions through the protoliths. According to Simons et al. (2017), zinc differs from 0.02 wt.% to 36.5 wt.% depending on its position; cadmium has high values over 1000 ppm, while indium content is up to 180 ppm locally. Minor cassiterite and sphalerite with chalcopyrite are intergrown with magnetite.

Treliver Minerals Ltd. (2015) reported that the inferred and indicated mineral resources of the Tellerhäuser deposit are estimated at 22.1 million ore tonnes with an average tin grade of 0.46% with a cut-off grade of 0.2% as of 2015. Thus, the deposit contains around 101,500 tonnes of tin. In the zinc and indium by-products calculation, 200,200 tonnes of zinc and 780 tonnes of indium were contained.

1.1.2 The Tellerhäuser processing pilot plant

In the scope of the “Processing of fine-grained polymetallic native Sn/W/In complex ores (AFK)” project, the characterisation and new beneficiation routes for fine-grained complex ore deposits in the Saxony region are aimed to be developed using modern simulations and current

analytical methods (Schach et al., 2021). Moreover, a pilot plant was installed to test the previously proposed processing route and to prove that such a process is economically feasible. Here 140 t of skarn ore from the Tellerhäuser deposit was processed in the pilot plant to process tin.

A flowsheet of the overall pilot plant is shown in Figure 1. It is divided into a non-continuous part containing different communition and classification steps and two-step XRT-sorting. Another aspect involves further communition, classification, and mineral separation units.

In the scope of the previous study (Schach et al., 2019), they produced sulphide concentrate through the flotation process. They removed impurities by several process stages, such as grinding and magnetic separation.

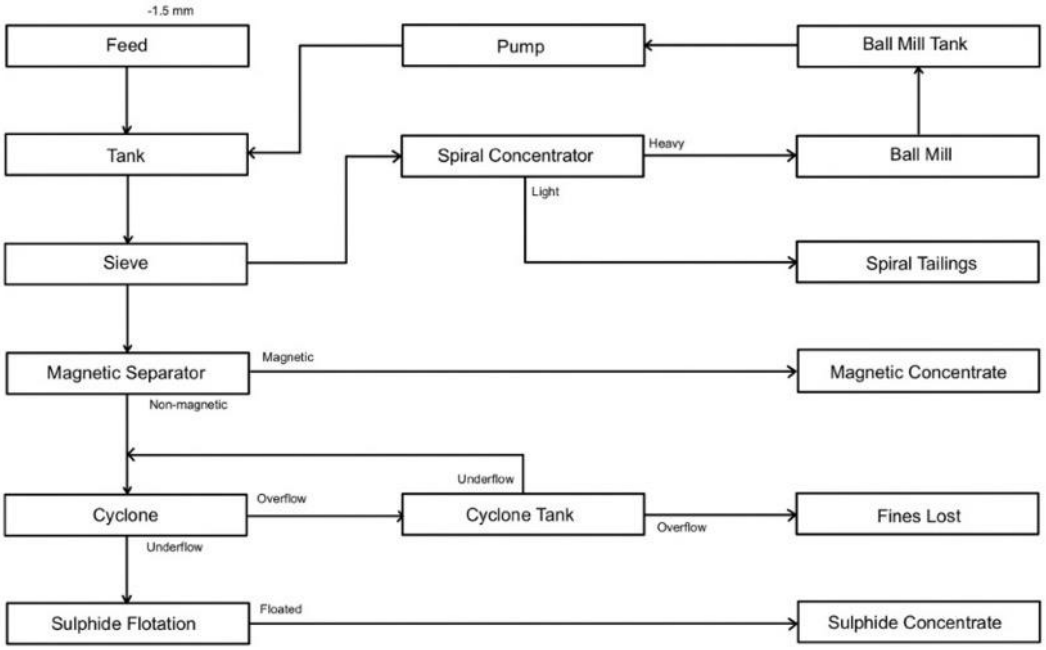

Figure 1. Flowsheet of the previous processes for producing sulphide concentrate from the Tellerhäuser pilot plant

A concentrate is rich in zinc, copper, and minor indium. In this sulphide flotation, xanthates were used as collectors and cupric ions as surface activators.

The sulphide flotation recovered 65,5% of the overall zinc at 41,8%, 37,7% of the copper at 0,8%, and 40,2% of arsenic at 2,3%. They also found that the sulphide concentrate contains a minor amount of indium here. Therefore, there is considerable economic interest in indium as a by-product since the concentrations in sphalerite are sufficiently high.

To develop a sustainable zinc recovery process, it is necessary to understand the mineralogy, determine the leachability of the metals, and investigate the recovery of valuable metals, not

only zinc but also trace elements such as indium, as well as gangue materials from the residues.

1.2 Main Goal(s) and tasks

The sole purpose of this thesis is to recover valuable metals from the sulphide concentrate, which was processed beforehand in the Tellerhäuser pilot plant, and to calculate the economic feasibility of the production of such metals. In order to achieve these aims, the research plan was divided into the following sub-objectives and tasks:

- Sample preparation for the further processing
- Investigation of direct acid leaching of the sulphide concentrate from the Tellerhäuser pilot plant with sulphuric acid and hydrogen peroxide
    - The leaching of multicomponent materials leads to the dissolution of various components. Hence it is crucial to understand the leaching behaviour and kinetics and the potential influencing parameters.
- Evaluation of the zinc and other valuable metals such as copper and indium extractability from the sulphide concentrate
- Evaluation of economic feasibility of the atmospheric leaching process
    - Possibility to scale up the leaching process to industrial scale
- Quantitative/Qualitative analyses of feed material and leaching solution, and leaching residue
    - The nature of the sample, its chemical composition, and mineral phases investigation will be studied.
    - The total concentration of the metals
- Discussion of the importance of this work and limitations

2 Theoretical background

2.1 Nature of zinc minerals

Zinc is the 24th most abundant element in Earth's crust. Zinc sulphide occurs naturally in sphalerite and wurtzite, which have different crystal lattices and frequently contain 5-15% iron. The primary zinc source is also sphalerite and is often intergrown with pyrite and pyrrhotite. It possesses some distinctive chemical properties; namely, it has relatively high resilience to external actions (Metz & Trefry, 2000).

A few zinc minerals can be considered for zinc production (Habashi, 1997) and are shown in Table 1. However, many studies used different sources than sphalerite, such as oxide-carbonate zinc ores (Dutrizac, n.d.), secondary materials such as leach residues (Ke et al., 2014; Turan et al., 2004), zinc dross (Ghayad et al., 2019; Rabah & El-Sayed, 1995; Wang et al., 2018), zinc ash (Ramachandran et al., 2004; Takacova & Trpčevská, 2010; Thorsen et al., 2014; Trpčevská et al., 2015), and flue dust (Asadi Zeydabadi et al., 1997; Barakat, 2003; Helbig et al., 2018; Thorsen et al., 2014) to extract zinc. These aggregates typically contain zinc and cadmium, copper, lead, silver, and iron.

Table 1. Common zinc minerals with their content(Habashi, 1997)

Mineral	**Formula**	**Zn content, wt. %**
Sphalerite, Wurtzite	ZnS	67,09
Hemimorphite, Calamine	$Zn_4Si_2O_7(OH)_2 \cdot 2H_2O$	54,30
Smithsonite Calamine	$ZnCO_3$	52,14
Hydrozincite	$Zn_5(OH)_6(CO_3)_2$	57,70
Zincite	ZnO	80,03
Willemite	Zn_2SiO_4	58,68
Franklinite		15-20
Sauconite		~35

2.2 Separation and concentration of sulphide ores

Most commercial zinc orebodies contain around 4% of zinc which is more than 20% in mass, although zones of pure sphalerite sometimes exist (Silin et al., 2020). Separation of zinc sulphide minerals from other sulphide minerals which are gangue is required, and it must be sufficiently concentrated by further processing.

Such techniques intend to reduce smelting costs and waste disposal at the smelter by reducing the number of wastes associated with mining. It is preferable to keep as much waste as possible in mine tailings.

Additionally, in order to meet the needs of a successful operation, zinc extraction processes typically require a particular range of zinc concentrates. As a result, the target specification in Table 2 (Sinclair, 2005) was used.

Table 2. Threshold of typical zinc concentrate composition for the zinc process (Sinclair, 2005)

Element	Composition range %
Zn	47 – 56%
Fe	< 10%
Pb	< 3%
Cu	< 2%
S	30 – 32%

Zinc ores have a wide range of properties and are frequently associated with complex minerals. To maximize separation efficiency, each deposit requires distinctive modified separation process.

These processes involve two main steps:

- Size reduction of the ore for total liberation and separation from one another. In this stage, zinc ores are usually beneficiated or concentrated by crushing and grinding.
- Froth flotation for selective physiochemical separation of individual minerals to improve the grade of the concentrate produced.

Fine grinding is a high-cost process in terms of both capital and operating costs. In some cases, it may not be viable to grind fine enough to produce satisfactory separation depending on the other possible factors in the mineral extraction processes (Sinclair, 2005).

Examples of the mineralogical and chemical compositions of materials from different sources are shown in Table 3.

Table 3. Mineralogical and chemical composition of materials from various sources - Example

Source	Mineral phases	Chemical composition, %	Reference
Sphalerite concentrate	Major: ZnS, Minor: FeS, Alumina, Silica	Zn – 49,50% S – 31,24% Fe – 9,66%	(Babu et al., 2002)
Sphalerite concentrate	Major: ZnS	Zn – 62,5% Fe – 1,063% Pb – 0,499% Insoluble SiO_2 – 3%	(Pecina et al., 2008)
Sphalerite concentrate	Major: (Zn, Fe)S Minor: $CuFe_2S$, FeS_2, PbS, SiO_2	Zn – 51,5% S – 23,14% Fe – 11,7% Cu – 0,63% Si – 1,2% Ca – 0,34%	(Picazo-Rodríguez et al., 2020)
Zinc leach residue		Fe – 13,6% Zn – 5,0% Pb – 5,4% Ca – 3,3% Cu – 0,26% Cd – 0,15%	(Ke et al., 2014)
Zinc dross		Zn – 96,18% Fe – 2,06% Al – 1,17% Si – 0,017% Pb – 0,007% Mg – 0,007% Ca – 0,02%	(Ghayad et al., 2019)

2.3 Zinc extraction processes

Possible zinc concentrate processing routes are compiled on the industrial scale and overviewed in Figure 2.

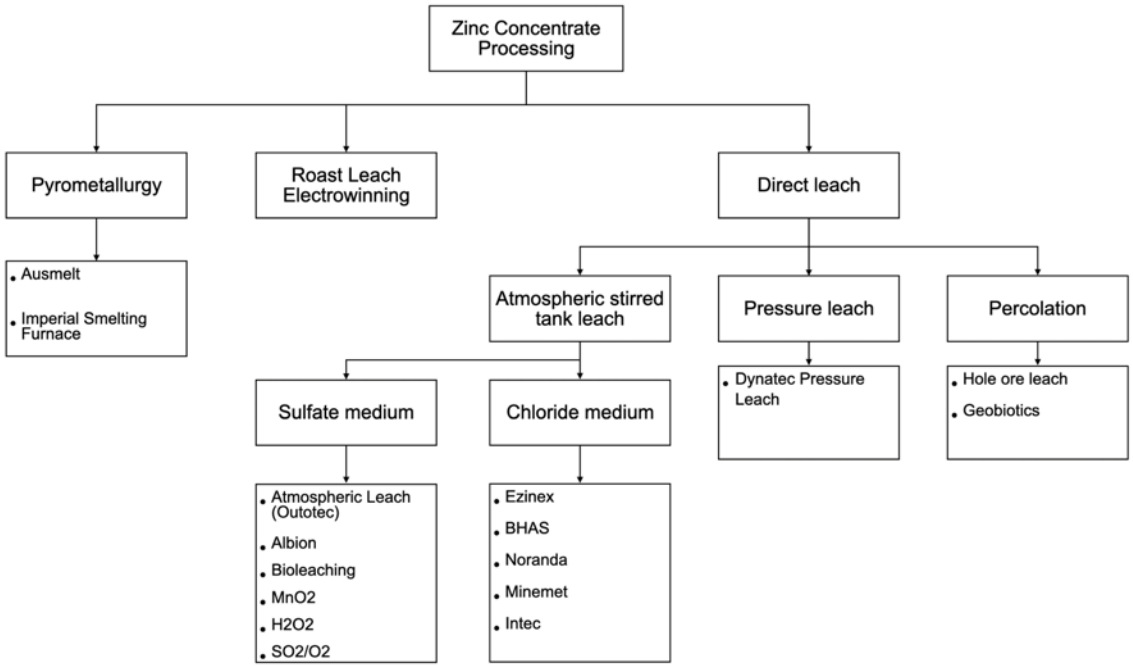

Figure 2. Overview of zinc sulphide concentrate process options

2.3.1 Pyrometallurgical processes

Zinc metal is produced by smelting zinc sulphide concentrate in pyrometallurgy. The most typical pyrometallurgical approach for zinc processing consists of the following stages:

- Roasting-sintering process of the zinc sulphide concentrates the zinc sulphide into an oxide.

$$2ZnS+O_2 \rightarrow 2ZnO+SO_2+ \text{energy}$$

- The zinc oxide produced is used in the imperial smelting process. In this stage, zinc fumes are condensed with the help of spraying liquid lead. Lead enriched in zinc is then cooled down to 450C at the condenser's outlet.
- The following process is called separation by liquation. In this process, refined zinc with a lead concentration, lead with a minor amount of zinc, and zinc matter of $FeZn_{13}$ crystals can be produced.
- The final stage is refining by distillation: At the exit of the columns, pure zinc enriched in low volatility elements such as Fe, Cu, and Pb is recovered.

2.3.2 Hydrometallurgical zinc extraction

Conventional methods for recovering zinc from zinc sulphide concentrate usually follow an electrolytic process. Over 85% of zinc production from sulphide concentrate or ores applies the roasting-leaching-electrowinning (RLE) process (Babu et al., 2002). The RLE flowsheet is shown in Figure 3. Typical RLE process flowsheet (Sinclair, 2005). Roasting is most conducted in a fluid bed roaster at 900-1000ºC.

Roasting of zinc sulphide concentrate produces acid-soluble zinc oxide (calcine) and sulphur dioxide, produced through the reaction of sulphur in the concentrate and air at above 900C in the same way pyrometallurgy. Consequently, sulphuric dioxide is converted to sulphuric acid in a recovery unit.

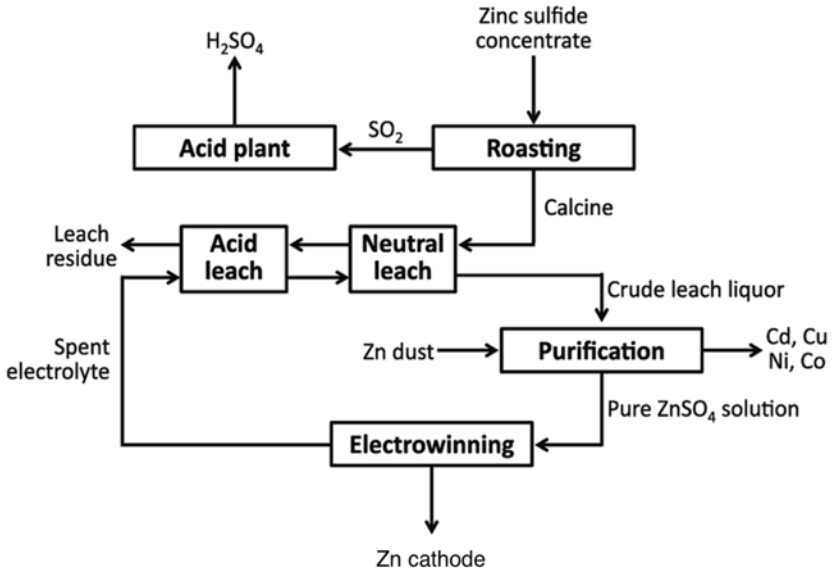

Figure 3. Typical RLE process flowsheet (Sinclair, 2005)

In the second stage, zinc oxide is dissolved in diluted sulphuric acid to produce a zinc sulphate solution. This leaching process is called neutral acid leaching. During this process, the impurities in the zinc concentrate can be leached simultaneously. Such presence of impurities can have detrimental effects on zinc production. Hence purification of the electrolyte is essential in the RLE process. These impurities strongly influence zinc electrowinning in the electrolyte. Many researchers (Anderson et al., 2014; Constantineau & Eng, 2004; Dimitrov et al., 2000; Kim et al., 2010) experimented on different parameters that may affect the recovery of zinc, such as temperature, particle size distribution, impurities of the material, use of other furnaces, residence time, and oxygen content to find the optimum conditions for maximising the zinc extraction.

There are issues related to roasting depending on the gangue materials inside the sulphide concentrate. In the RLE process, the zinc sulphide fraction reacts with the iron impurities by

forming zinc ferrite ($ZnFe_2SO_4$). Zinc ferrite is one of the biggest problems for hydrometallurgical processes because of its highly stable structure and insolubility in dilute sulphuric acid, alkaline, and chelating media under such conditions (Balarini et al., 2008). On the other hand, basic sulphates are formed in the roasting of zinc sulphide above 400C. The reason for zinc ferrite formation is also lower partial pressure of oxygen than the required amount for zinc oxide formation (Shamsuddin, 2021b).

From the economic viewpoint, the pyrometallurgical route demands high-grade ores or concentrates on saving thermal energy in heating the gangue and slagging. In contrast, the grade of ore or concentrate is not essential in the hydrometallurgical method, and it is still profitable on the feeds, which are uneconomical to be treated by pyrometallurgy. Besides, the equipment used in the hydrometallurgical plants is simple and relatively cheap, and thus, it can be built at a low capital cost (Shamsuddin, 2021a). In hydrometallurgy, the reagents used during leaching experiments can be easily regenerated; and after the process, zinc needs refining and can be used directly for alloy making.

2.4 Direct leaching

The direct leaching of sphalerite concentrates aroused great interest over several years because the roasting is eliminated in this process (Babu et al., 2002; Mubarok et al., 2018; Picazo-Rodríguez et al., 2020; Sadeghi et al., 2016; Sinclair, 2005). There are more distinctive advantages to the direct leaching process compared with the RLE process; for instance, the process can be used for small-scale operations without high investment; high zinc recovery is achieved by consuming relatively low energy.

However, there are disadvantages such as a lack of recovery of the exothermal heat from the roasting stage and the requirement for disposal of sulphur residues for environmental reasons.

2.4.1 Leaching mechanisms

The leaching process follows heterogeneous reactions between the reagent and the solid. This transformation can be described by the shrinking core model illustrated in Figure 4. In this

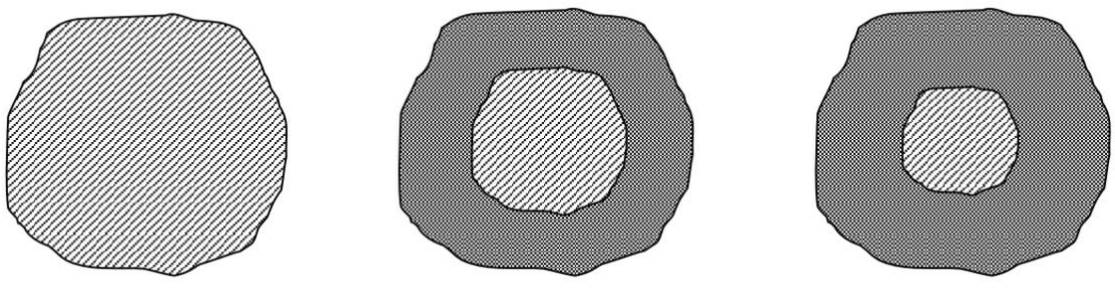

Figure 4. Shrinking core model for leaching

model, the gas or liquid first reacts with the reactant material at the surface, and then the sulphur as one solid product of the reaction remains. The size of the unreacted core decreases as the reaction progresses.

While there are a variety of leaching reagents available, sulphuric acid is the most common and practical. Sulphuric acid is a highly reactive reagent that can dissolve iron, aluminium, zinc, manganese, magnesium, and nickel in diluted form.

The following equation represents this process with sulphuric acid:

$$ZnS+H_2SO_4=ZnSO_4+H_2S(aq)$$

Sulphuric acid, on the other hand, is not suited for processing carbonate and magnesium-rich zinc ores because the acid consumption is too large, and the magnesium result is too difficult (Safari et al., 2009).

Two direct leaching processes have been suggested for zinc sulphide direct leaching: high-pressure with high temperature and atmospheric leaching process.

In most cases, oxygen in a sulphuric medium is used to carry out the zinc extraction process in hydrometallurgy.

The presence of oxygen in the system decreases the sulphuric acid attack effect in direct leaching processes. Sphalerite could be oxidised directly by pressured oxygen and sulphuric acid as follows:

$$2ZnS(s)+O_2+2H_2SO_4\rightarrow 2ZnSO_4(aq)+2H_2O+2S\ (s)$$

Due to its slow kinetics, selecting an oxidising agent suitable for hydrometallurgical zinc recovery from sphalerite concentrate has been considerable attention. Possible oxidants that can be considered in such a process and their equilibrium redox potential are listed in Table 4.

Various oxidants such as ferric ions (Ghassa et al., 2017), ozone (Mubarok et al., 2018), hydrogen peroxide (Aydogan, 2006; Picazo-Rodríguez et al., 2020), ammonium, and sodium and potassium persulphate (Babu et al., 2002; Sahu et al., 2006) were studied to overcome this shortcoming in the sulphide material leaching.

Table 4. The equilibrium redox potentials of different oxidising agents with respective reactions

Oxidising agent	Redox potential, V	Reaction
O_3	2.07	$O_3+2H^++2e^- \rightarrow O_2+H_2O$
$K_2S_2O_8$	2.00	$S_2O_8^{2-}+2e^- \rightarrow 2SO_4^{2-}$
H_2SO_5	1.81	$SO_5^{2+} +2H^+ 2e^- \rightarrow SO_4^{2-} + H_2O$
H_2O_2	1.77	$H_2O_2 + 2H^+ + 2e^- \rightarrow 2H_2O$
$KMnO_4$	1.49	$MnO_4^-+ 8H^+ +5e^- \rightarrow Mn^{2+} + 4H_2O$
NO^+	1.45	$NO^+ + e^- \rightarrow NO\ (g)$
$NaClO_3$	1.45	$ClO_3^- + 6H^+ + 6e^- \rightarrow Cl^- + 4H_2O$
Cl_2 (g)	1.358	$Cl_2\ (g) + 2e^- \rightarrow 2Cl^-$
$K_2Cr_2O_7$	1.33	$Cr_2O_7^{2-} + 14H^+ + 6e^- \rightarrow Cl^- + 4H_2O$
O_2 (g)	1.23	$0.5O_{2\ (aq)} + H^+ + 2e^- \rightarrow 2H_2O$
HNO_2	1.202	$NO_2^- + 2H^+ + e^- \rightarrow NO_{(g)} + H_2O$
MnO_2	1.20	$MnO_2 + 4H^+ + 2e^- \rightarrow Mn^{2+} +2H_2\cancel{O}$
HNO_3	0.957	$NO_3^- + 4H^+ + e^- \rightarrow NO_{(g)} + 2H_2O$
Fe^{3+}	0.77	$Fe^{3+} + e^- \rightarrow Fe^{2+}$
Cu^{2+}	0.153	Cu^{2+}/Cu^+

2.4.2 Direct acid pressure leaching

Direct acid pressure leaching has been commercially used in many zinc ore, and zinc concentrate leaching plants (Filippou, 2010; Ozberk et al., 1995) and has been investigated in several studies(Gu et al., 2010; Xie et al., 2007); it is also an alternative to the conventional RLE route. In this process, zinc sulphide is directly leached and forms elemental sulphur, thus, zinc production does not depend on sulphuric acid consumption.

Figure 5 depicts common processes of direct pressure leaching. In autoclaves, the leaching is carried out at higher pressure and temperatures than in open leaching tanks. When using gaseous reagents, high-pressure leaching is desirable. Sphalerite could be oxidised by pressured oxygen and sulphuric acid as follows:

$$ZnS+H_2SO_4+\frac{1}{2}O_2 = ZnSO_4+H_2O+S^\circ$$

According to Sinclair (2005), lead and other metal sulphides oxidise the same way zinc sulphide does. The rate of the reaction mentioned above is low. Although the presence of iron in the solution dramatically enhances the rate of attack regardless of the pressure level, in other words, it can be used as an oxidising agent in direct acid leaching at atmospheric pressure. This shows that the following reaction is of most importance:

$$ZnS+Fe_2(SO_4)_3 = ZnSO_4+FeSO_4+S^\circ$$

For most circumstances, acid-soluble iron in zinc concentrates is adequate to meet the process's requirement for iron ions; however, ferric sulphate more than the stoichiometric amount does not fasten the reaction. Consequently, the behaviour of iron in the autoclave is monitored by the acid content in the leach solution.

High-pressure leaching is beneficial when gaseous reagents such as oxygen and ammonia are involved (Shamsuddin, 2021a). The most significant advantage of oxygen gas compared to other reagents is that it has no harmful effect on the environment. However, one of the main challenges of this process is that it is performed at a temperature above the sulphur melting point (115ºC). Therefore, the liquid sulphur may spread rapidly throughout the surface of unreacted mineral particles, which results in a decrease in the rate of metal dissolution. Even though direct pressure leaching enables fast concentrate dissolution, some problems are found in operation and maintenance of autoclaves due to high pressure. Moreover, this process is capital-intensive since an elevated temperature and pressure are needed. Atmospheric leaching is considered an option to address the issues encountered in industrial pressure leaching processes.

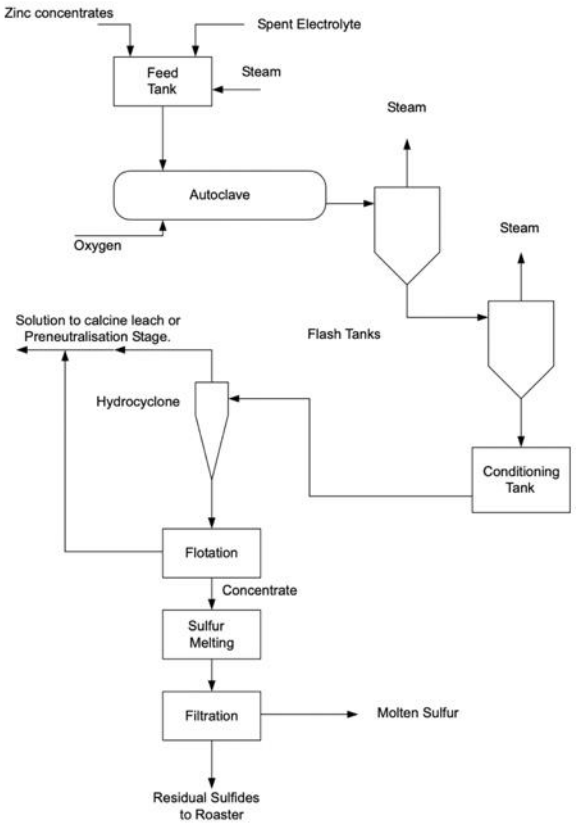

Figure 5. Typical flowsheet of direct pressure leaching

2.4.3 Direct acid leaching at atmospheric pressure

For decades, direct acid leaching has been used on an industrial scale for zinc recovery from zinc sulphides. This process is like low-temperature (<100ºC) and pressure (< 1 atm) leaching since it is operated under oxygen-rich conditions. In this process, the zinc concentrates are oxidised in acid media in the presence of different oxidising agents. Moreover, due to lower maintenance costs, direct atmospheric leaching is less expensive than the direct pressure leaching process. However, this process is characterised by slow dissolution kinetics requiring around 24h for leaching, while only 1,5 hours of residence time are needed for the pressure leaching process under the same conditions (Filippou, 2004).

In this process, pH must remain below 2 to avoid iron hydroxide precipitation (Sinclair, 2005). From another perspective, the impurities can be removed by adjusting pH. Minor impurity elements such as arsenic, antimony, aluminium, germanium, indium, and gallium can be co-precipitated with iron into the iron residence. Thus, it is crucial to control the pH if the by-product of the leaching is one of these metals mentioned previously.

Using oxygen

Among chemical oxidisers, adding oxygen as an oxidising agent of atmospheric leaching was a little more desirable option. A reactor was invented suitable for the direct atmospheric leaching of zinc sulphide concentrate. It consists of a tube with an oxygen inlet and stirrer (Sadeghi et al., 2016).

The presence of iron in sphalerite minerals significantly influences the dissolution rate. Ferric ion can be used to leach sphalerite according to the following reaction:

$$ZnS+2Fe^{3+} \rightarrow Zn^{2+}+2Fe^{2+}+S^{0}$$

Using hydrogen peroxide

Hydrogen peroxide is used to form a high redox potential of 1.77 V, which is sufficient to oxidise almost all the metal sulphide in an acid medium and pressure when it decomposes to produce oxygen gas.

According to Aydogan (2006), the oxidation action of hydrogen peroxide in an acid medium is based on its reduction as follows:

$$H_2O_2+2H^{+}+2e^{-} \rightarrow 2H_2O$$

Another important aspect is the stability of hydrogen peroxide. In acidic solutions, it is relatively stable without any homo- or heterogeneous catalysts. Nevertheless, trace amounts of inorganic cations, the rise of temperature or concentration, and pH increase decomposition

rate. Notably, iron and copper in the solution lead to rapid disproportionation (Nicol, 2020). This instability is the main drawback of hydrogen peroxide in the leaching system.

The oxidation reaction of sphalerite in an acid solution (pH<2) entails the dissolution of the mineral. The reaction forms metal ions and elemental sulphur.

$$ZnS \rightarrow Zn^{2+} + S^{\circ} + 2e^{-}$$

The following reaction with the overall equation being:

$$ZnS + H_2O_2 + 2H^{+} \rightarrow Zn^{2+} + S^{\circ} + 2H_2O$$

The reactivity of the sphalerite itself varies significantly and can be related to the amount of contained iron; the higher this is, the higher the reactivity (Sinclair, 2005). Reaction rates are considerably lower than direct pressure leaching; long residence time is required.

Using ammonium persulphate

When ammonium persulphate is used as an oxidant with sulphuric acid to oxidise zinc sulphide as in the following reaction:

$$ZnS + (NH_4)_2S_2O_8 \rightarrow ZnSO_4 + (NH_4)_2S_2O_2 + S$$

According to Sahu et al. (2006), it was found that the recovery of zinc increases with the temperature rise. However, when the temperature was above 60ºC, the extraction decreased due to early decomposition. The recovery also increased up to 95% when fine particles were less than 45 µm due to the correlation of ferric concentration with temperature over time. The kinetics shows that the rate is governed by mass transport of the oxidant through the mineral surface layer. The strength of this study compared to others is that a maximum temperature has been identified, which, if exceeded, results in a reduced recovery. This finding helps future studies focus on lower temperature technologies to achieve high recovery while consuming less energy.

Using manganese dioxide

The addition of manganese dioxide ore to a sphalerite concentrate has effectively dissolved both zinc and manganese due to the formation of two corrosion couples in a sulphuric acid medium. A further possibility exists of dissolving sphalerite in the presence of manganese dioxide via galvanic contact; both dissolves as follows:

$$ZnS \rightarrow Zn^{2+} + S + 2e^{-}$$

$$MnO_2 + 2HCl \rightarrow MnCl_2 + Cl_2 + 2H_2O$$

This study has concluded that non-oxidative dissolution and the cyclic action of converting ferric to ferrous ions do not contribute considerably.

Table 5. Direct acid leaching conditions with different oxidising agents and leaching yields

Oxidising agent	Leaching medium	Particle size	Temperature	Leaching time	S/L ratio	Leaching yield	Reference
H_2O_2	5% H_2SO_4	-38 µm	60ºC	4h	50g/L	Zn – 80%	(Pecina et al., 2008)
APS	H_2SO_4	-45µm	60ºC	5h	100g/L	Zn – 95%	(Sahu et al., 2006)
0,5M Fe^{3+}	0,5M H_2SO_4	-70µm	80ºC	5h	50 g/L	Zn – 95% Cu – 19% In – 95% Sn – 28%	(Santos et al., 2010)

2.4.4 Leaching kinetics

Since leaching is an interactive process between dissolved reagents and the solid phase, it is crucial to determine the affecting parameters for the leaching rate. Numerous process parameters can influence the leaching rate based on the rate-determining step.

If the leaching is chemical reaction-controlled, the factors can conjecture from the reaction rate of a heterogeneous reaction with a constant acid concentration as follows:

$$-\frac{dW}{dt} = k \cdot A \cdot C$$

Where W is the particle's weight at the time, t; k is the rate constant; A is the particle's surface area, and C is the concentration of the reactant.

From here, the rate constant k is dependent on temperature. Moreover, the particle's surface area will also affect the reaction rate F, concluding from the equation above.

On the contrary, if the leaching process is diffusion-controlled, the diffusion rate will be described as follows:

$$D = \frac{RT}{6\pi r \eta N}$$

Where D is diffusion; the universal gas constant R; T is temperature; r is particle radius; η is the substance's viscosity, and N is Avogadro’s number. Therefore, the rate is affected by the temperature and size of the particle in the diffusion-controlled system.

Further, mineralogy can be a governing factor in understanding the leaching mechanism and predicting the leaching rates of minerals. Due to their various, chemical, and physical features

may exhibit drastically different behaviour. Sulphide leaching in an acidic medium result in a decrease in leaching rate with time. This was obtained by forming a reaction product on the mineral surface, hindering further leaching. Some literature (Forero-Saboya et al., 2020; Hackl et al., 1995) mentioned that there are the following issues concerning the nature of the passivation layer:

- A slow rate of transfer of electrons and ions
- Transfer of ions from the electrolyte to the surface or vice versa
- The entire coating of the surface and prevention of attacking oxidants from contacting the active sulphide mineral surface.

As a result, the porous sulphur layer is formed on the surface of the sulphide mineral. The pH also significantly affects leaching kinetics because it influences the yield of chemical reactions, producing different mineral formations according to their value range.

3 Materials & Methodology

In this chapter, the materials used and the experimental work carried out in this study. The experimental work consists of sample preparation and characterisation of the samples for different analyses shown in Figure 6. In the end, the experimental setup and procedure of leaching experiments will be described.

3.1 Materials and reagents

This study used solely analytical-grade chemicals and reagents provided by Merck,

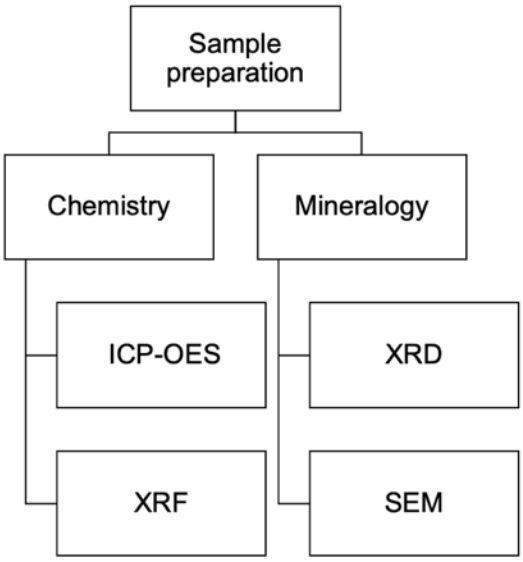

Figure 6. Flow diagram of analysis methods for sample

AcrosOrganics, and Carl Roth. Table 6 shows the list of chemicals and materials used throughout all experiments. The primary reagent of the leaching experiment is sulphuric acid; hydrogen peroxide was selected as an oxidising agent in this study. All solutions were made using deionized water; and the samples for Inductively Coupled Plasma-Optical Emission Spectroscopy (ICP-OES) were diluted with 1% nitric acid. Acid digestion experiments were carried out with 67% nitric acid and 37% hydrochloric acid.

The feed material in this study is a bulk concentrate of sulphide flotation in the previous pilot plant to process 150 t tin skarn ore from the Erzgebirge region, Germany. The tin skarn ore contains considerable tin, zinc, indium, and other valuable metals. As a result of the pilot plant, a total mass of 89,331 kg sulphide concentrate was produced. The sulphide concentrate has been stored in the form of sludge for over two years in the storage room of HIF. The initial condition of the concentrate is seen in Figure 7a.

Table 6. Lists of reagents used in the leaching experiment

Reagent	Formula	Application	Concentration
Sulphuric acid	H_2SO_4	Main reagent	AR with a concentration of 96%
Hydrogen peroxide	H_2O_2	Oxidising agent	AR with a concentration of 30%
Nitric acid	HNO_3		AR with a concentration of 67%
Hydrochloric acid	HCl		AR with a concentration of 37%

3.1.1 Leaching test

Sample preparation

The sulphide concentrate has been crushed and ground beforehand. The material, which was obtained using froth flotation, was initially wet, and therefore it was dried in the oven at 105ºC before being deagglomerated and homogenized. Figure 7a depicts the initial state of the wet bulk sulphide concentrate and dried agglomerate material. The dried material was split into smaller portions using sample divider Retsch PT 100 and Retsch PT 600 as required for the various analyses and main experimental work (see Appendix I). In some leaching tests, size reduction was required. As a result, materials were wetly milled in a rod mill, then dried again at 105ºC in the oven before being dry screened in size fractions of 50+80 µm and -50 µm. The fractions were stored in small plastic bottles and labelled.

For simplicity of use, 2M H_2SO_4 was freshly prepared before every leaching experiment by diluting the analytical grade of sulphuric acid and was stored in a 1000 ml bottle. Since the hydrogen peroxide was added for over 48 hours, the storage condition was adjusted to preserve the solution as suitable as possible. To do so, 250 ml brown glass bottles were used

Figure 7. (a) Feed material at its initial condition and (b) Feed material after drying at 105°C

to keep it from light; however, the temperature for the solution was 24 ±1ºC which was not ideal for 30% hydrogen peroxide. The bottles were tightly sealed and kept in the fume hood.

Samples were prepared for the ICP-OES analysis. The total metal content of the samples was determined by aqua-regia digestion. A volume of 4,5 ml of 37% HCl and 1,5 ml of 67% HNO_3 was added to around 200 mg of a solid sample and placed into a vessel. The vessels were put into microwave Anton Paar Multiwave 5000 and were heated to 230ºC with a maximum power of 773 W and a maximum current of 11,4% for 30 min, and then were cooled to a temperature of 70ºC for 30 min. Then, deionized water was added until the total volume reached 50 ml. Then the liquid samples were centrifuged, and the solid and liquid were separated. The final solution was analysed for the following metal concentrations: Zn, In, Fe, As, Sn, and Cu.

Leaching setup

The leaching experiments were carried out in a 1l Tralero & Schlee Mini reactor, with a mechanical agitator for providing proper mixing electric heating. It is equipped with a thermometer for temperature control and a cooling system to maintain the set temperature, as illustrated in Figure 8. Furthermore, an additional pump was installed between two reactors and was connected to the reactors to allow for a slower input of hydrogen peroxide. All batch reactors were checked and cleaned thoroughly and properly before starting new experiments.

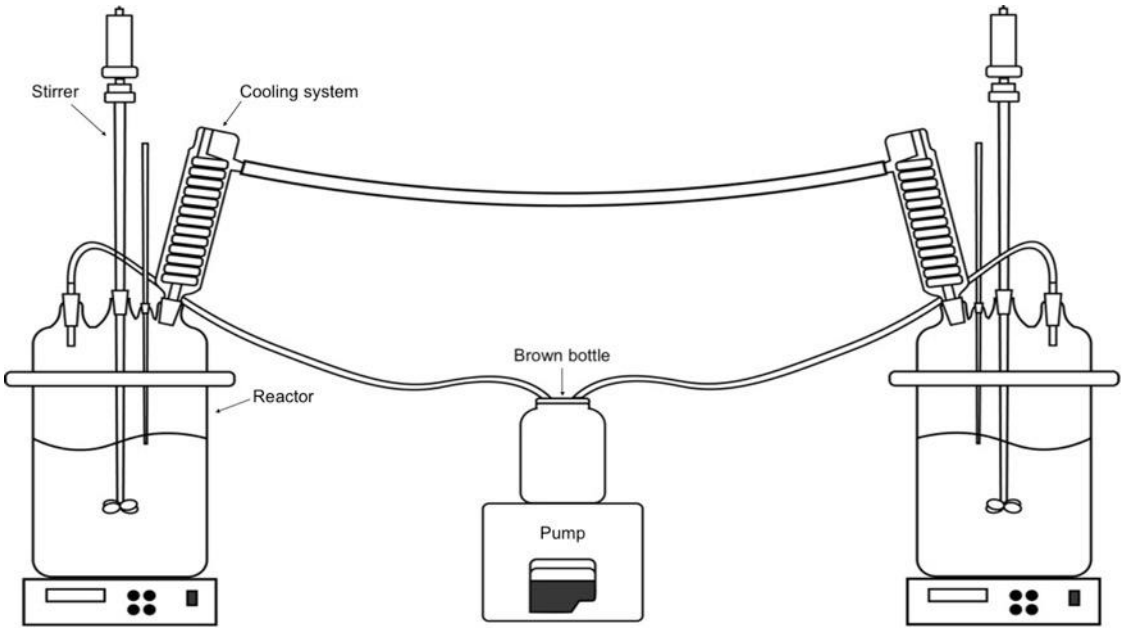

Figure 8. Experimental set-up for leaching with H_2O_2

Experimental procedure

The experiments were performed with sulphide concentrate, sulphuric acid, and an oxidising agent in the reactor. The pump for the addition of hydrogen peroxide was placed between two

reactors. All leaching experiments were carried out with the same procedures to ensure precise results.

Depending on the number of sulphuric acid concentrations to be investigated, different volumes of 2M sulphuric acid were introduced to the reactors, and the deionized water was added accordingly. 30% hydrogen peroxide was added to a separate brown bottle, which kept hydrogen peroxide out of the light, and the amount of 30% hydrogen peroxide was regulated by the concentration required for each leaching experiment. Table 7 lists the parameters for the performed experiments.

The solution in the reactor was preheated until it reached the required temperature. 80 g sulphide concentrate was submerged in a solution containing 2M H_2SO_4 and deionized water. Moreover, 30% H_2O_2 was added constantly by a pump with a rate of 2.4ml/h during the experiment. The process was mainly carried out with a duration of 96 hours. All the experiments were performed with a total volume of 800 ml of leaching solution (S/L = 1:10) and a stirring speed of 340 rpm.

5 ml aliquots were withdrawn at regular time intervals for chemical analysis. Then they were centrifuged and split into supernatant from suspended solids. The metal concentrations in each new sample were determined by ICP-OES. The pH was measured at the end of the leaching by a pH meter ALMEMO 2590-2A/-4AS.

After each leaching experiment, the solution was filtered by a vacuum pump with filter paper. The filter paper was weighed and placed into a funnel. Then, leach solution was poured into the filter paper to separate pregnant leach solution from solid leach residue. The leach residue was put into a vacuum oven at room temperature to avoid any changes to sample properties and prevent any other new phase formation for 48 hours. After drying, the filter cake was removed from the range and weighed again to determine the weight of each leach residue to calculate moisture. Once the weight of each leach residue was calculated, the residues were separately stored and kept for further analyses. It was analysed by X-ray diffraction (XRD) with X-ray diffractometer PANalytical Empyrean (r=240 mm), Scanning Electron Microscope (SEM) with scanning electron microscope FEI Quanta 650F MLA-FEG used for Mineral Liberation Analyzer (MLA) to explain the behaviour of solids during the leaching process under different conditions.

Metal extraction (E in %) was calculated as follows:

$$E = \frac{c_i^t \cdot V^t}{m \cdot w_i} \cdot 100\%$$

where c is a concentration of element i in leaching solution after leaching time t (in mg/L) $V^t$is a volume of the leaching solution after leaching time.

3.2 Modelling and design of experiments

The experimental design was used to screen the parameters and construct a numerical model to find the optimum conditions for the leaching process. The experimental error was calculated by duplicating the central point. The experiments were carried out in a random order to decrease the impact of systemic errors. Preliminary experiments were carried out at three different temperatures: room temperature, 40ºC, and 60ºC with 0.5M sulphuric acid for 168 hours to choose the temperature as a set parameter. There were experiments to find an effective method for adding hydrogen peroxide: adding 6 ml H_2O_2 with a pipette and constant addition with a pump with the slow rate mentioned above to slow the decomposition of hydrogen peroxide. In the H_2SO_4-H_2O_2 system, different acid concentrations and hydrogen peroxide concentrations were investigated; further experiments are designed and summarized in Figure 8.

Table 7. Experimental conditions

Experiment	Leaching medium	Oxidising agent	Method of adding an oxidising agent	Temperature control	S/L ratio	Leaching time
Temperature control	0.5M H_2SO_4 (2.68%)	No	No	varied	1:10	168h
Addition method of H_2O_2	0.5M H_2SO_4	5% H_2O_2	Varied	40ºC	1:10	168h
H_2SO_4 - H_2O_2 system	H_2SO_4	H_2O_2	With pump	40ºC	1:10	96h

Table 8. Experimental design - varied parameters

Parameter	Unit	Parameter levels			
H_2SO_4 concentration	mol/L	0.3	0.5	1.0	1.5
H_2O_2 concentration	%	1	3	5	
Particle size	µm	D_{90}< 150	+50-80	-50	

3.3 Characterisation techniques

Three different size fractions of the bulk sulphide concentrate were characterised. As a characterisation, the physical characterisations of all three size fractions were done to determine the particle size distribution. The chemical composition of the feed was evaluated using ICP -OES at both Helmholtz Institute Freiberg and TU Bergakademie Freiberg and X-ray Fluorescence (XRF) at Helmholtz Institute Freiberg. Then the mineralogical characterisations of each sample were done by XRD and SEM. The data obtained by SEM was processed through Mineral Liberation Analyzer (MLA). The results of the analyses mentioned above will be given in the following subsections.

3.3.1 Chemical characterisation

The feed sample was analysed for target elements for ICP -OES: Zn, Cu, Fe, As, Sn, and In. The data obtained from XRF was used to select elements of interest throughout this study. The elements chosen were evaluated reactions of interest concerning the aims of this study: sulphide oxidation and the dissolution kinetics of sulphide concentrate. Some elements were not studied due to their low concentrations on the feed. After the leaching experiment, the elements analysed on the solid residues and leachates are also the same as the interest elements analysed on the feed. The leachates were analysed by ICP-OES, while XRF analysed leaching residues due to incomplete digestion.

The different feed samples (-50 µm, -80+ 50 µm, and bulk feed) and residues were analysed by XRF equipment, a PANalytical X-fluorescence spectrometer with an Energy Dispersive Minipal 4 (Rh X-ray tube 30kV -9W) at a resolution of 150 eV.

After the leaching, the samples were centrifuged using a centrifuge machine; the liquid was separated from suspended matters. It was essential to ensure no suspension of particles in the liquid sample for ICP-OES analysis. 2ml of the sample was pipetted into a 5 ml tube and was made up to 4 ml by diluting with 1% HNO_3 to 2 times.

3.3.2 Mineralogy

SEM was used to investigate the mineralogy and grain characteristics of the feed sample at Helmholtz Institute Freiberg. It provides quantitative mineralogical data from particle maps. It also distinguishes minerals and calculates data such as modal mineralogy, bulk geochemistry, and mineral associations of samples as a function of density, chemical properties of mineral and measured surface with the assistance of MLA.

In SEM, a high-energy beam is focused on the solid sample where signals are created. These signals give information about the texture, chemical composition, and crystalline structure of the sample. This also enables the production of tomographic data using 3D imaging.

SEM analyses were performed on the representative samples of the concentrate (leach feed) and its leach residue. The concentrate was characterised using this technique. The samples were embedded in epoxy, and then the cured blocks were reduced to size and exposed using a diamond cutting wheel. They were then polished and carbon-coated before being subjected to the tests. The mineralogy of particles was determined using SEM data. MLA grain-based X-ray mapping (GXMAP) approach was chosen as the measurement model for the analysed sample. Minerals are consistently detected because their grayscale (BSE mode) is used to distinguish them.

In addition to the SEM, bulk mineralogy was validated using XRD at Helmholtz Institute Freiberg. XRD is a fast analytical technique primarily used for mineral identification of crystalline materials by providing information on peaks at various angles. XRD functions by having rays interfering with the crystal sample surface. A cathode-ray tube produces these X-Rays, filtered to produce monochromatic radiation. When Bragg's Law is met, the sample interacts with light rays to produce constructive interference.

The samples from the feed materials and the leaching residue were ground into refined grains. The feed samples were then dried at 105°C, while the leaching residues were dried in vacuum conditions at 22°C and 21 mbar for 16 hours.

PANalytical Enpyrean diffractometer was used with Co X-ray tube anode with the following measurement settings such as 35kV voltage and 35mA current with an iron beta-filter operating at scan range: $5\text{-}80^{0}$.

4 Results & Discussions

4.1 Feed sample characterisation

4.1.1 Particle Size Analyses

Laser Diffraction Sensor (LDS) was used to determine the particle size distribution of different materials which were dry milled with various milling times; the LDS result is presented in Appendix II. Based on the result, the most efficient milling time was 5 minutes; therefore, the bulk feed material was milled for 5 minutes and then screened to -50+80 µm and -50 µm to test the effect of mineral beneficiation, before the leaching, on the metal extraction.

After that, the particle size distribution of all three feed materials (bulk, 50+80 µm, -50 µm) was analysed by MLA. Figure 9 depicts that around 80% of the bulk feed passed through 125 µm sieve. In general, feed materials contain a relatively high number of fine particles.

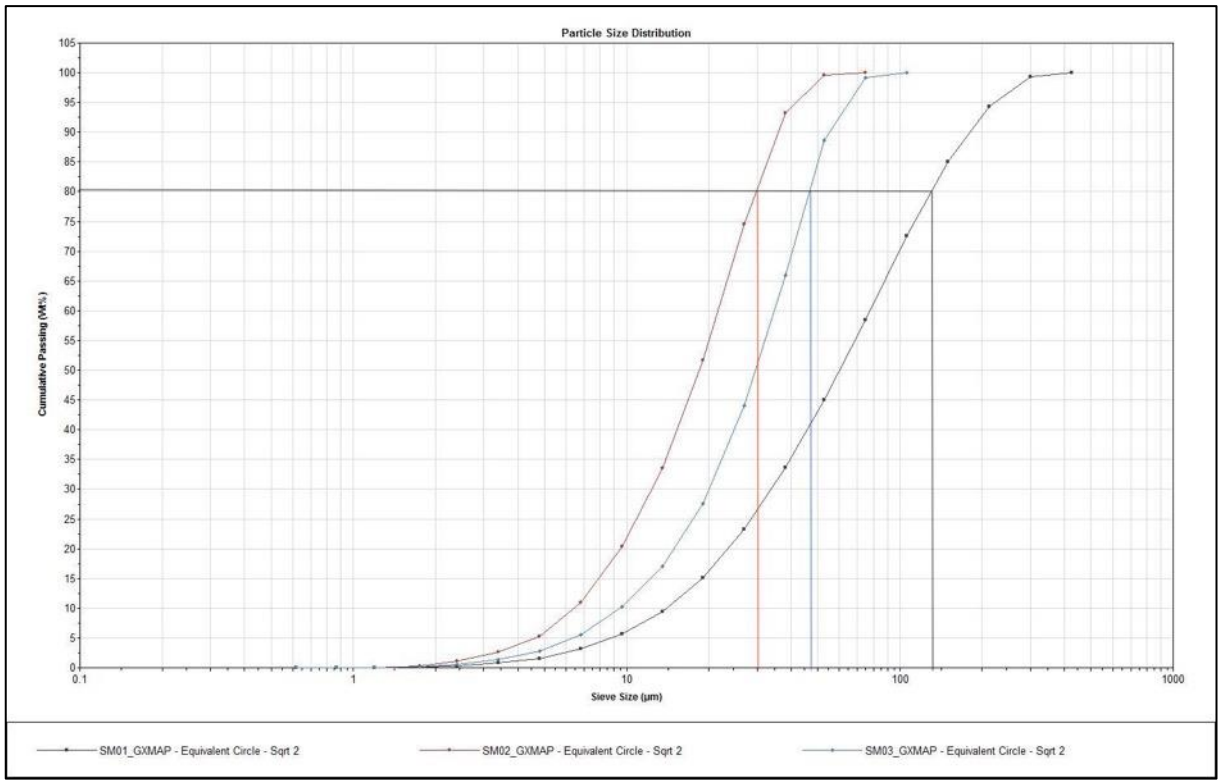

Figure 9. Particle size distribution curve of three different feed materials (obtained by MLA)

4.1.2 Elemental analysis

The chemical composition of the feed material is critical for determining the metal extraction rate of each leaching experiment; hence it is essential to achieve an accurate chemical composition of the feed material. The assays of target metals in three distinct feed materials were measured by ICP-OES, XRF, and MLA; the results were summarised in Table 9. All feed

materials contain a high amount of Zn (41-45 wt.%), a significant amount of Fe (12-15 wt.%), As (1-2 wt.%), Cu (1-1,5 wt.%), as well as a minor amount of In (< 100 ppm) and Sn (<200 ppm).

To begin with the ICP-OES result, the samples for ICP-OES were acquired because of the microwave-assisted acid digestion method in aqua regia to determine concentrations of the main target elements. However, some solid matters, presumably silicate, contained minerals such as quartz and feldspar, as insoluble phases were present after the digestion and then suspended from the solution. Therefore, the result from the ICP-OES analysis may not be accurate for the trace elements such as indium and tin. Each feed sample was digested at least three times; the result represents the average of the three experiments with minor deviations.

Following that, the solid feed samples were analysed using the XRF method to identify the complete elemental composition of the feed. Although the composition is not oxide, the initial XRF results are usually given in the form of oxides. As a result, it had to be recalculated using the elemental forms using their atomic masses. The conversion of oxide forms to elements can be imprecise due to the availability of various sources for the element's chemical properties. Unfortunately, the XRF method is ineffective for detecting trace elements. In this case, it did not detect indium in the feed because of its trace amount.

Table 9. Chemical composition of three different feed materials with various analyses

Assay, %	Bulk			+50-80µm			-50 µm		
	ICP-OES result	XRF result	MLA result	ICP-OES result	XRF result	MLA result	ICP-OES result	XRF result	MLA result
Zn	43,8	44,47	43,86	44,7	48,4	43,2	41,7	41,7	41,3
Cu	1,29	1,36	1,07	1,3	1,3	1,3	1,37	1,47	1,3
In	0,08		-	0,04	-	-	0,02	-	-
Fe	12,39	13,85	15,13	12,6	13,8	15,5	12,7	15,0	16,1
As	1,47	1,33	1,34	1,57	1,51	1,7	1,7	1,7	1,8
Sn	0,03	0,23	0,16	0,08	0,18	0,19	0,03	0,27	0,3

At last, the samples were sent to SEM analysis for assistance with MLA which calculated the chemical assays based on the elemental mapping from SEM. As is the case with XRF, this technique incapable of quantifying the trace elements. Moreover, the result is not suitable for calculating the dissolution rate, but it supports in comparing it to the other results obtained through different analytical methods. All chemical composition results have mostly minor deviations on each element. This demonstrates the reliability of the results. However, the ICP-OES results were used for further calculations since the concentration of the leaching solutions

was analysed by the same methods. The results, including additional elements, can be found in the Appendix III.

4.1.3 Mineralogical analysis

Feed samples were characterised using XRD and SEM-EDS-based image analysis. XRD analysis was used to reconcile data regarding modal mineral content, while SEM-EDS supplied more accurate mineralogical and textural data extracted from particle maps.

It is important to note that all Zn-bearing minerals found in the thin sections are shown in Figure 11. From the result, sphalerite was the main host of Zn in the studied samples. Over 93% of the sphalerite in the feeds were >90 % liberated; in other words, this amount of sphalerite can contact directly with leaching reagents. It could be seen that the size reduction tends to create more free surfaces for leaching.

The mineralogical compositions of the feed materials acquired by XRD are shown in Appendix IV. The measurement of the bulk material showed that the main mineral phases were sphalerite and was detected the presence of arsenopyrite, chalcopyrite, pyrite, quartz, and k-feldspar, which is consistent with the findings of Schach et al. (2021).

However, XRD analysis does not show all minerals inside the feed material, and its detection limit is strongly phase-dependent and quantification of the abundance of minor minerals (< 3,0 wt.%); therefore, MLA data are taken into account for the mineralogical composition (Table 22) of all three feed materials. Minerals were grouped wherever suitable to simplify without compromising the distinctive characteristics of the various lithological units. Modal mineralogy

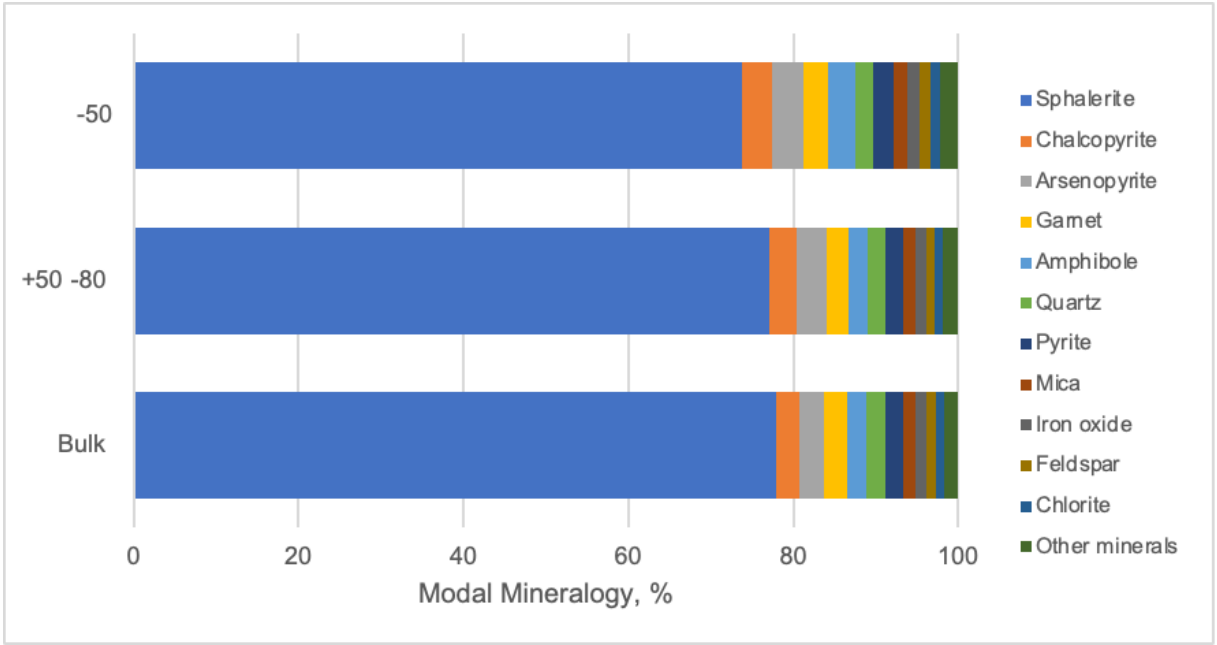

Figure 10. Modal mineralogy of the grain mounts from the feed sample with different size fractions

of the feed materials is illustrated with modified mineral groups in Figure 10, which shows that the main mineral phase is sphalerite (70-80 wt.%), and there are different types of sulphide minerals in them.

The Zn deportment is defined as the quantitative distribution of the total Zn content of the ore among the major Zn host minerals. The mineralogical composition result has also shown several sphalerites with different iron content. Therefore, it was decided to divide them based on their iron content. These findings indicate that sphalerite is the dominant host of the measured Zn content in all three feed material samples. Figure 11 shows that approximately 50% of sphalerite in the feed contains up to 15% iron. It can also be seen that sphalerite in this study has a much higher iron content. It is also worth noting that a trace amount of Zn was detected inside minerals other than sphalerite; however, the minerals that do not host Zn contained a trace amount of Zn. The contamination can be explained by flotation reagents from previous processes in the Tellerhäuser pilot plant.

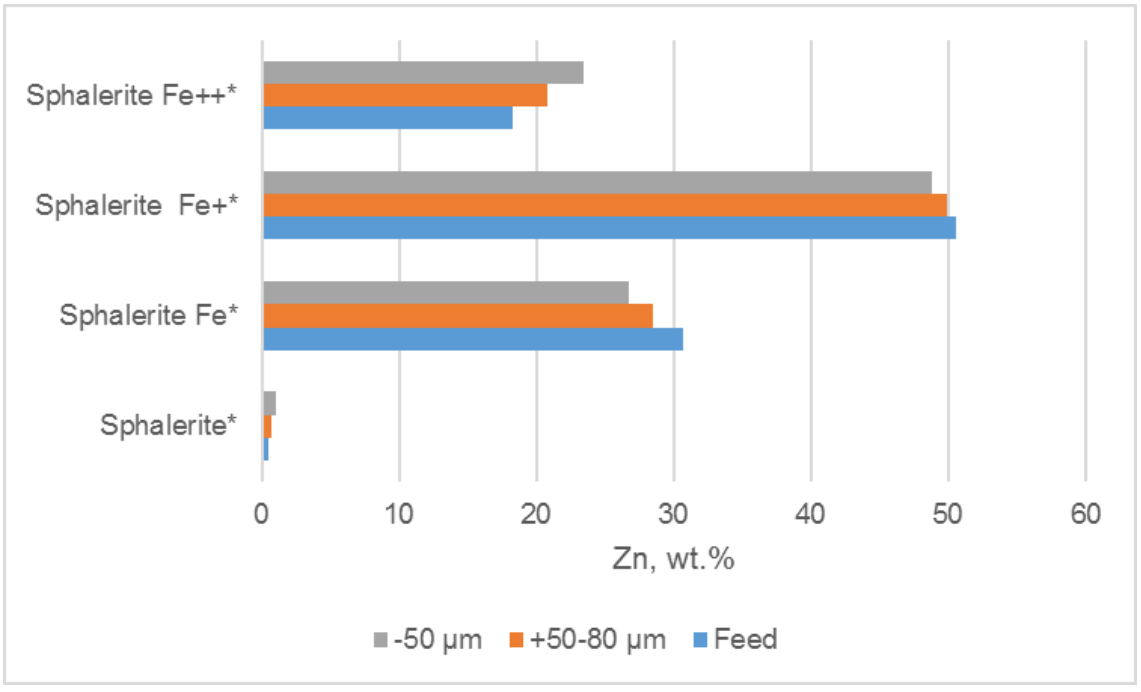

Figure 11. Zn deportment of feeds with different size fractions. Sphalerite*; Sphalerite Fe* (Fe~5%); Sphalerite Fe+* (Fe~15%); Sphalerite Fe++* (Fe~20%)

4.2 Direct acid leaching with hydrogen peroxide

In all experiments, the stirring speed remains constant due to the previous research (Aydogan, 2006), which shows a very slight effect of stirring speed on the metal extraction at any leaching time. In order to avoid any solid material from adhering to the sides of the reactors, which may lead to less contact time of solids with solution, the optimum stirring speed was set at 340 rpm. It only affects the part of the reaction which is physically controlled.

The leaching curves may be divided into two stages. In the first stage, which occurs up to the first 48 hours of reaction, the kinetics of metal dissolution is relatively fast, whereas the second stage presents a much lower leaching rate.

4.2.1 Effect of temperature

Experiments were undertaken to investigate the effects of various leaching temperatures on the leaching behaviour of the sulphide concentrate. Zinc extraction results are plotted as a function of time in Figures 12 &13. The effect of temperature is investigated using different size fraction materials. The experiments were under three temperatures: a) room temperature (24 ºC), b) 40ºC c) 60ºC. Due to the decomposition of hydrogen peroxide, previous studies (Antonijević et al., 1997; Mahajan et al., 2007; Sahu et al., 2006) suggested setting the temperature under 60ºC.

In theory, increasing the temperature in the leaching system will result in faster leaching kinetics. Figure 12 shows how temperature affects the extraction of zinc without any other variable which also includes no addition of hydrogen peroxide in the system. After 96h extraction rate was 11% at 60ºC and significantly higher than at 40ºC (5%). At room temperature there was almost no Zn extraction was observed. Nevertheless, we can see that zinc extraction increases with increasing temperature.

The effect of temperature was thus investigated with a solution containing 0.5M H_2SO_4 and an oxidising agent (5% H_2O_2) pumped for over 2 days. The overall trend is depicted in Figure 13. In all cases, Zn extraction rapidly increases at the start of the experiment and slows down after 48h which can be attributed to decreasing amount of zinc sulphide, the formation of a layer of sulphur or the stop of the addition of hydrogen peroxide. In contrast to the previous experiment and the result for the bulk material, the highest extraction rates could be observed at the temperature of 40ºC for the two other size fractions. For instance, the zinc extraction from +50 -80 µm after 96h was 64,0%, 85,8%, and 76,8% at room temperature, 40ºC, and 60ºC, respectively.

Hence, the subsequent experiments/investigations were carried out at 40ºC in the extent of the temperature chosen. In preparation for the reactors to reach their designed temperature, they were preheated at 40ºC for 10 minutes. At the end of this period, the solid samples were added to the reactors, and the actual experiment time started. This was performed to reduce possible errors.

The oxidation of S^{2-} regulates the entire process of electron and protons transfer within the solid structure, as well as ferric ion diffusion to the interface.

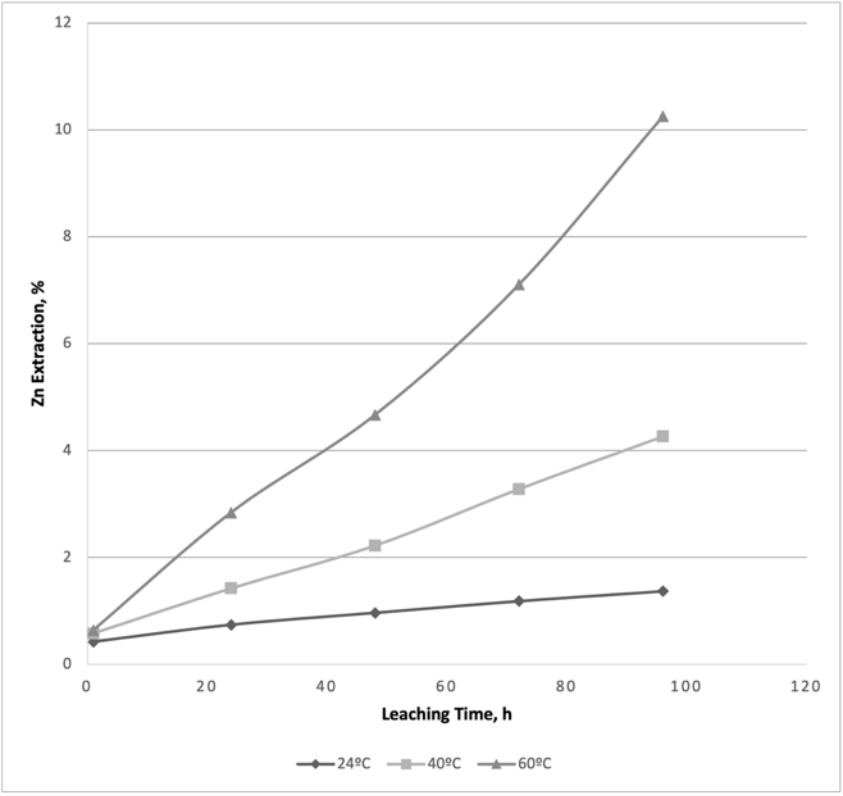

Figure 12. Effect of temperature on zinc extraction (bulk material; 0.5M H_2SO_4)

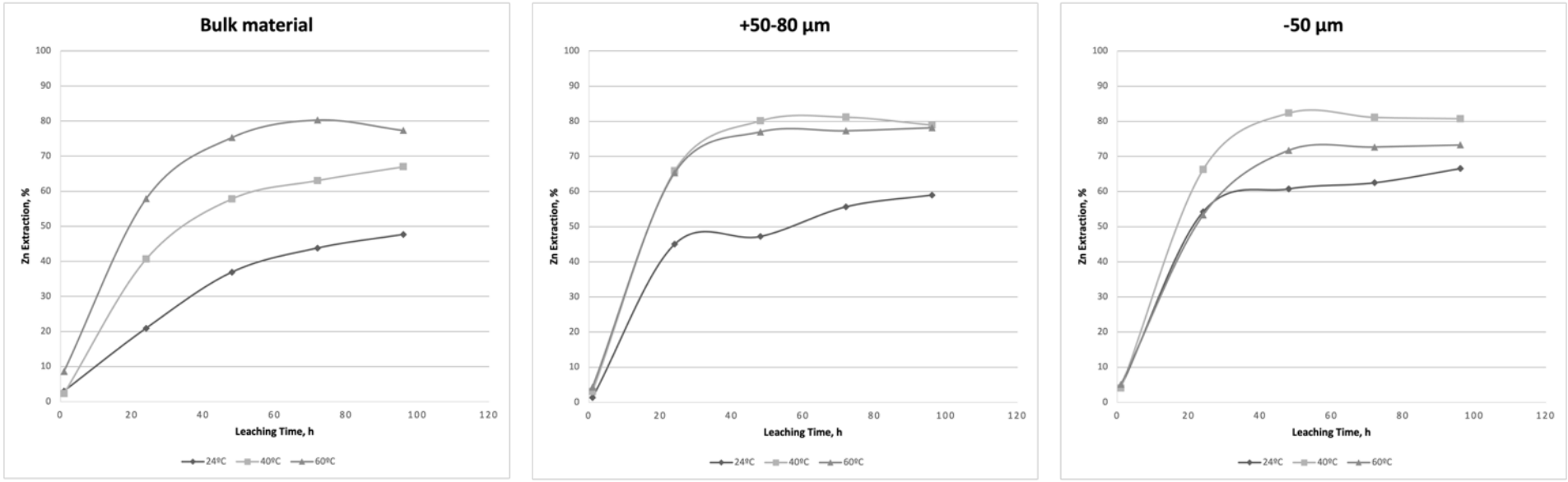

Figure 13. At different temperatures a) with bulk material b) with +50-80 micrometer fraction c) -50 micrometer fraction – at 0.5M H_2SO_4 and 5% H_2O_2 pumping

4.2.2 Effect of acid concentration

In order to investigate the influence of the concentration of sulphuric acid on the extraction rates of Zn and other metal ions (Fe, Cu, As, Sn, and In). Sulphuric acid concentrations of 0.3M, 0.5M, 1.0M, and 1.5M were tested on all different size fractions at 40C, with 5% H_2O_2 and pulp density (1:10 w/v).

Figure 14 depicts the extractability of Zn, As, Cu, Fe, Sn, and In for all acid concentrations. From this, it could be observed that Zn and Fe were continuously increasing when increasing acid concentration, whereas As and Sn were extracted only when more than 1M H_2SO_4. Moreover, the result showed that In extraction is at its maximum at 1M H_2SO_4; however, the Cu extraction rates did not show an increase when varying the acid concentration.

To be more specific, it shows that a low H_2SO_4 concentration is favourable to minimize the gangue metals extraction so that they can remain in the residue. However, a low acid concentration also leads to poor extraction of valuable metals, in this case, Zn and In.

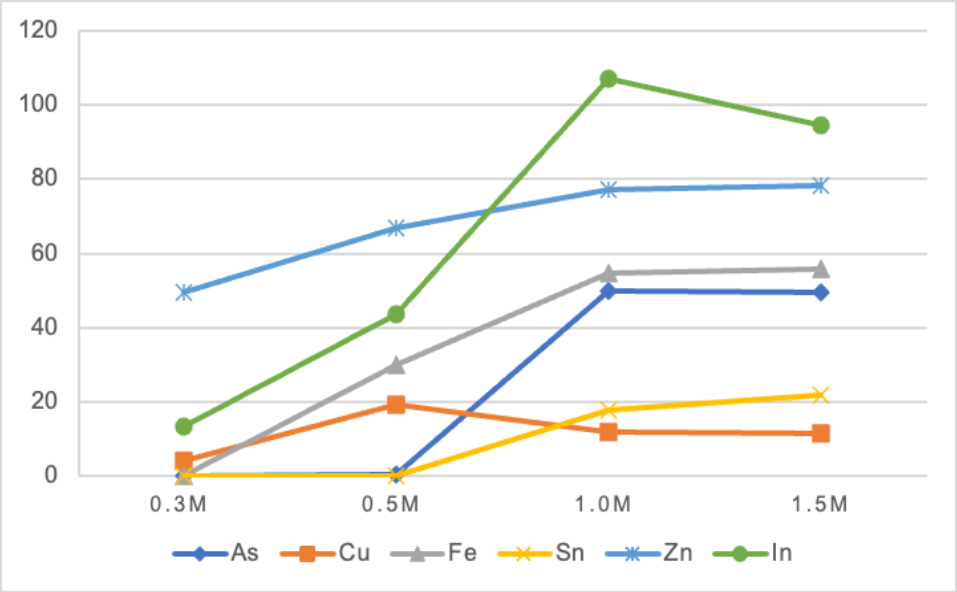

Figure 14. Effect of acid concentration on different metal extraction - at 40°C with 5% H2O2

For 0.5M H_2SO_4, the maximum zinc extracted is 66,6%, while 1.0M H_2SO_4 has achieved 76.6%. These results can be explained by the increase in the redox potential of the oxidant; the hydrogen ion concentration increases the redox potential of hydrogen peroxide, which consequently increases the reaction rate (Picazo-Rodríguez et al., 2020).

After these experiments, the variation in zinc extraction is plotted in Figure 17. It is shown that zinc extraction increases as the acid concentration increases. The zinc extractions after 96 h leach at 0.3M and 1.5M H_2SO_4 were 50,52% and 79,73%, respectively. This suggests that H_2SO_4 significantly influences sulphide concentration to extract zinc.

From Table 10, the pH levels of the experiments indicate the strength of the acid, and it positively affects zinc sulphide dissolution.

Table 10. pH value on varying acid concentration

Size fraction	Temperature	Oxidant concentration, %	Acid concentration, M	pH value
Bulk	40	5	0.3	4,7
			0.5	2,49
			1.0	0,78
			1.5	0,32

According to the pH measurements, the pH values after leaching are higher than before leaching. In general, higher sulphuric acid concentrations result in faster rates and increasing zinc extraction rates.

The effect of acid concentration has a misleading result on the leaching rate of iron. As seen in Figure 15, iron extraction rises when acid concentration occurs. The result may vary due to the high solubility of ferric sulphate in a highly acidic solution. The hydrolysis of iron in the solution is depicted by the acid concentration in the leaching system. Moreover, Figure 15 depicts the precipitation of iron minerals when acid concentration is 0.3M and 0.5M.

Effects on different metals

Generally, indium is predominantly associated with sphalerite. However, arsenic and indium presented similar behaviour in an acidic medium. From Figure 16, arsenic and indium were precipitated at lower acid concentrations. In other words, it is possible to precipitate arsenic and indium by adjusting the pH of the solution. The selective precipitation of arsenic can be achieved at a pH of 2.5 and 3.5 (Lalancette et al., 2012).

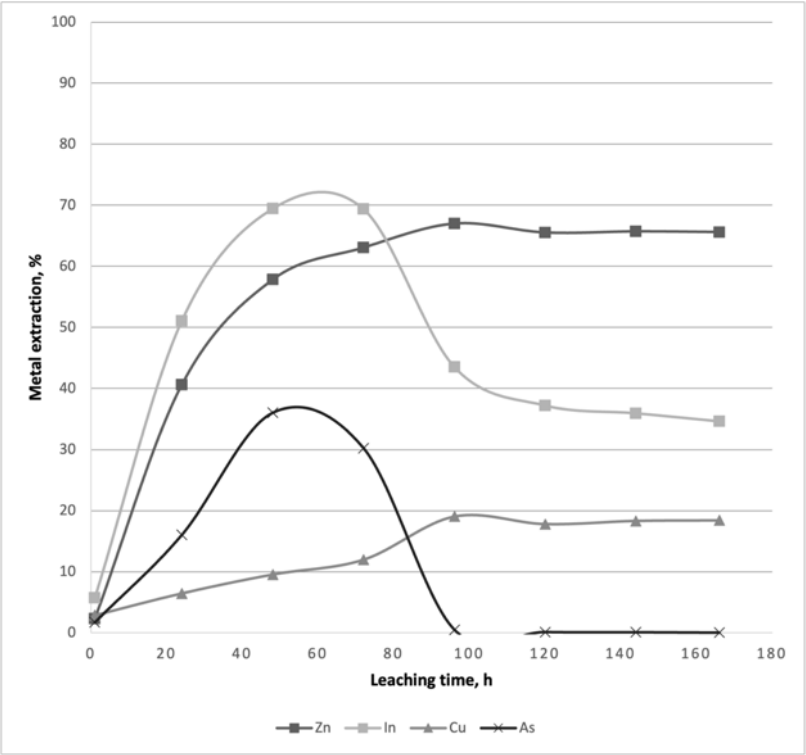

Figure 16. The behaviour of different metals with 0.5M H2SO4 at 40°C (bulk feed material, 5% H_2O_2 pumping)

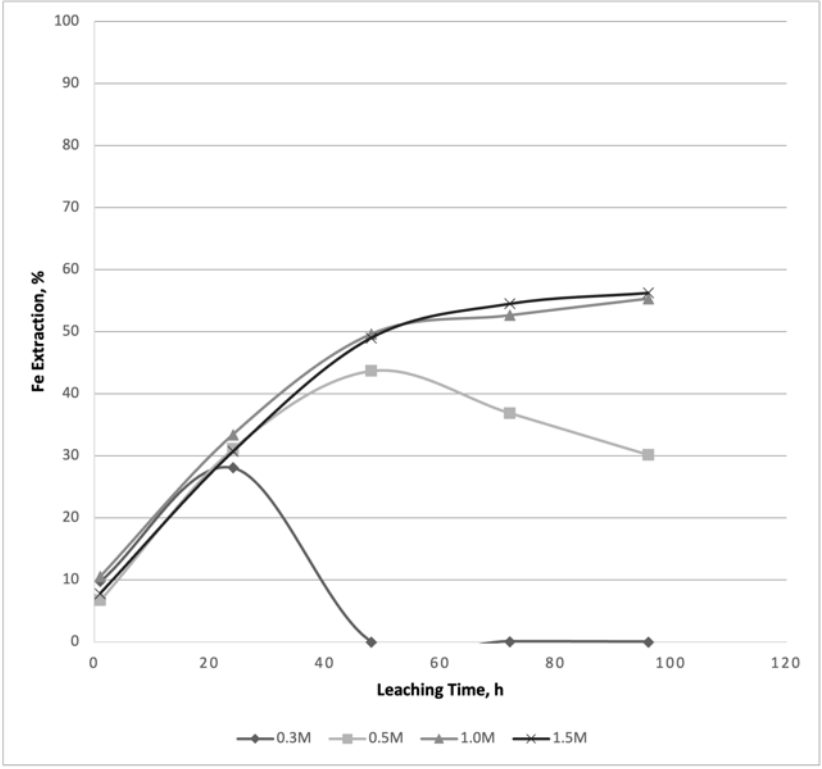

Figure 15. Effect of acid concentration on iron extraction at 40°C with 5% H_2O_2 pumping

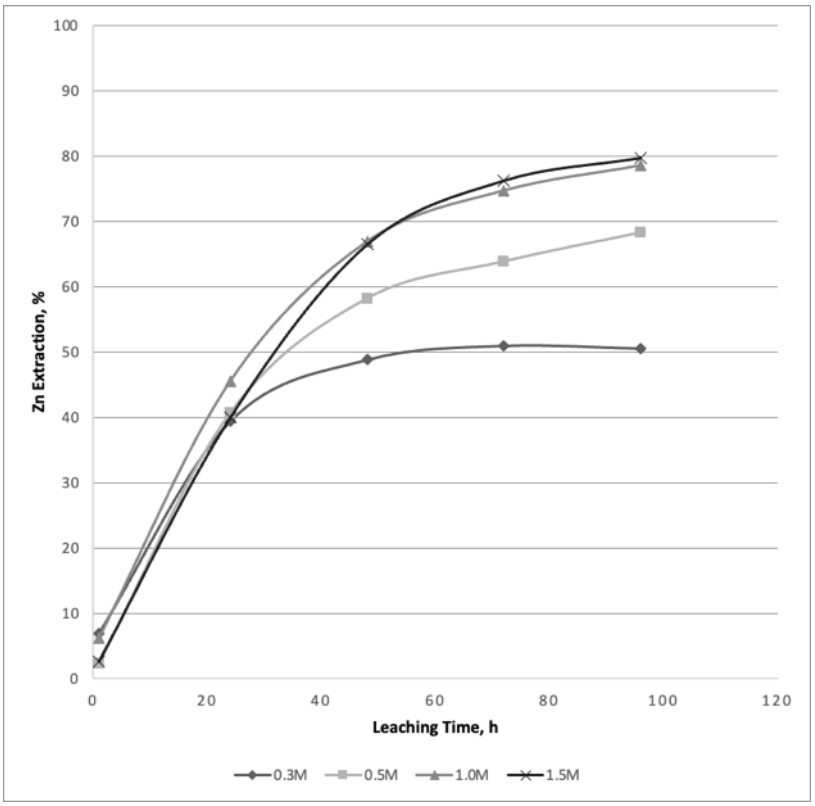

Figure 17.Effect of acid concentration on zinc extraction at 40°C with 5% H_2O_2 pumping

4.2.3 Effect of particle size

Two samples were measured at each milling time to prove the samples were homogenous. Based on the particle size needed in the leaching experiment and the size distribution, the most suitable milling time was 5 minutes.

The influence of particle size on zinc extraction was investigated in the range of bulk material to -50 µm in a solution containing 0.5M H_2SO_4 with and without 5% H_2O_2. Results are shown in both Figure 18 and Figure 19 which illustrate that the overall zinc dissolution is higher for the finer particles than the coarse particles at room temperature. Reducing particle size benefits zinc extraction and leaching time reduction. This behaviour was expected from the mechanism where a chemical reaction and diffusion mainly control the dissolution through a porous film. The zinc may become more exposed to the solution, which allows the zinc for leaching when milled.

The effect of fine grinding has a significant impact on the diffusion-controlled dissolving process. However, smaller fractions show almost no difference in the zinc extraction at 40ºC in such conditions. Thus, it can be concluded that pre-treatment for the concentrate increases the metal extraction; however, it is crucial to find the optimum size fraction to increase milling effectiveness and reduce the milling time, which is one of the critical parameters for energy consumption. The zinc extraction reached 66,7% for bulk sulphide concentrate, whereas it reached 81,3% for the fine size fraction of the concentrate after 96 h.

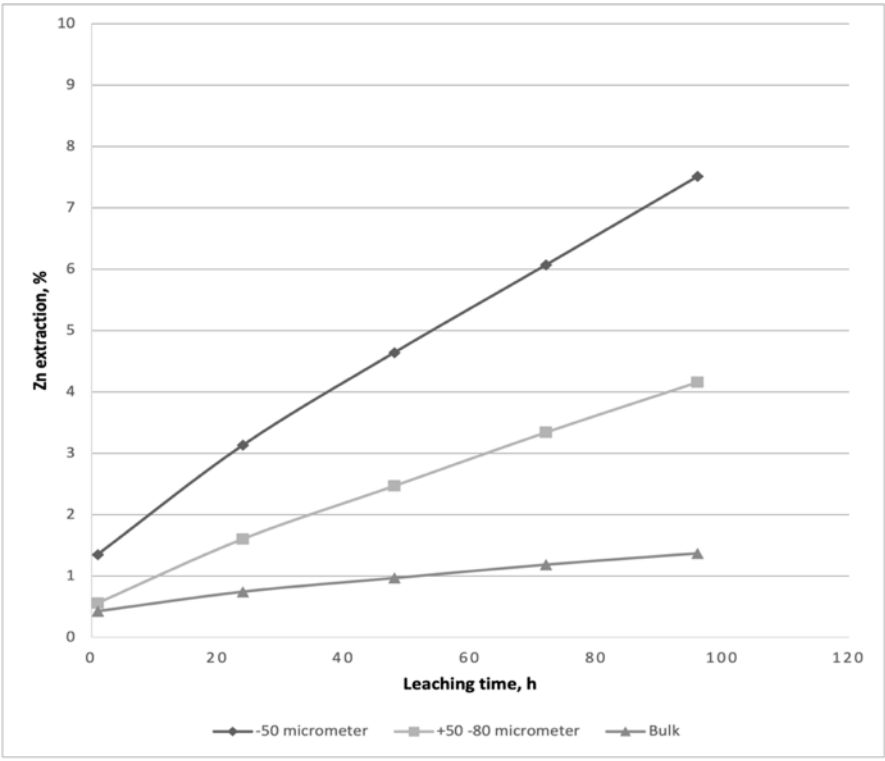

Figure 18. Effect of particle size on zinc extraction (24°C, 0.5M H_2SO_4)

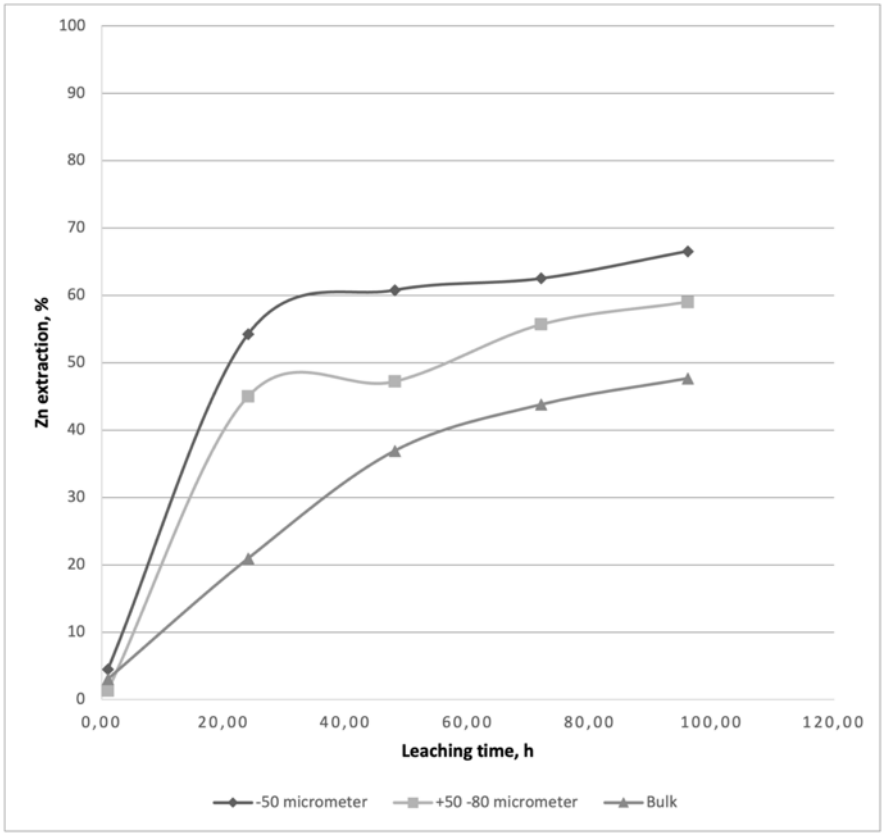

Figure 19. Effect of particle size on zinc extraction (24°C, 0.5M H_2SO_4, 5% H2O2)

4.2.4 Effect of oxidant concentration

Hydrogen peroxide was used as an oxidising agent to improve the kinetics of the reaction. It is considered a strong agent for its redox potential in an acid medium. In the first experiments, H_2O_2 was added by a pipette for over 1 hour. However, there was a significant temperature increase; and the formation of the bubble was observed during the addition, which can be seen in Figure 20b. It was, therefore, necessary to control H_2O_2 addition into the leaching system slower but constant by using a pump.

The results of different methods of H_2O_2 addition are shown in Figure 21. Here it can be seen clearly that pumping H_2O_2 has a much more significant effect on zinc extraction. After 96 hours, the zinc extraction reached 25,2% when H_2O_2 was added by a pipette every 5 minutes for over an hour, while it reached 68,3% when a pump added H_2O_2 for over 48 hours. Therefore, all further experiments were carried out with the pump.

Moreover, various hydrogen peroxide concentrations at 1%, 3%, and 5% were examined at baseline conditions to compare the effects. The results of the zinc extraction from the bulk sulphide concentrate are illustrated in Figure 22. The zinc production is higher at 5% compared to other concentrations observed. This can be explained by the dissolved oxygen reacting at the mineral surface to form metal ions. Previous studies have shown that the increase in hydrogen peroxide concentration increased the recovery of zinc; however, the metal extraction

Figure 20. a) before adding H_2O_2 b) after adding H_2O_2

rate significantly decreased when hydrogen peroxide concentration was over 5%. Overall, increasing the hydrogen peroxide concentration increases the extraction to a certain extent.

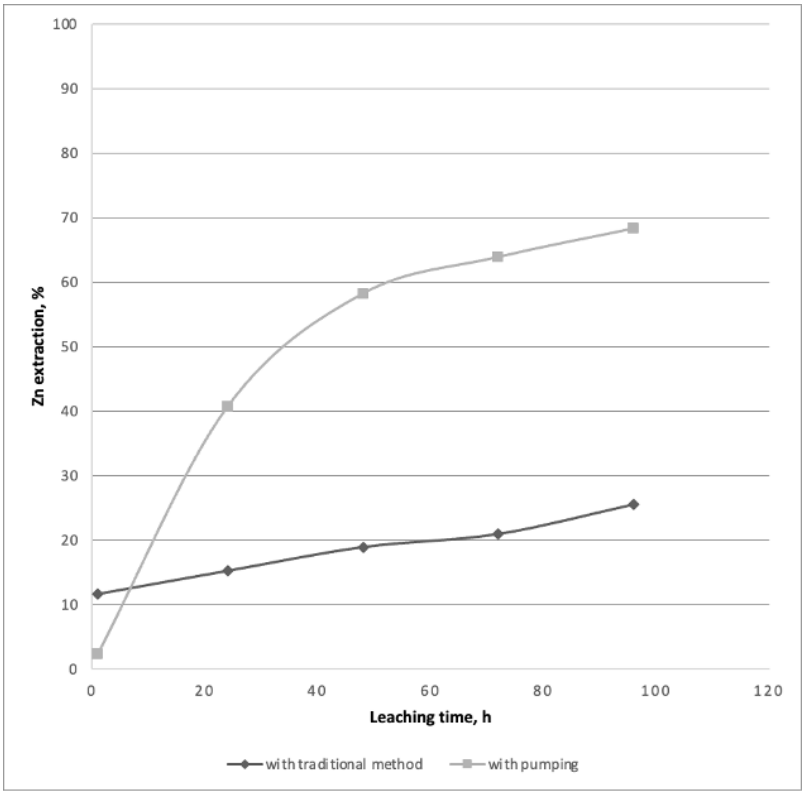

Figure 21. Comparison of methods of H_2O_2 addition with 0.5M H_2SO_4 and 5% H_2O_2 at 40°C

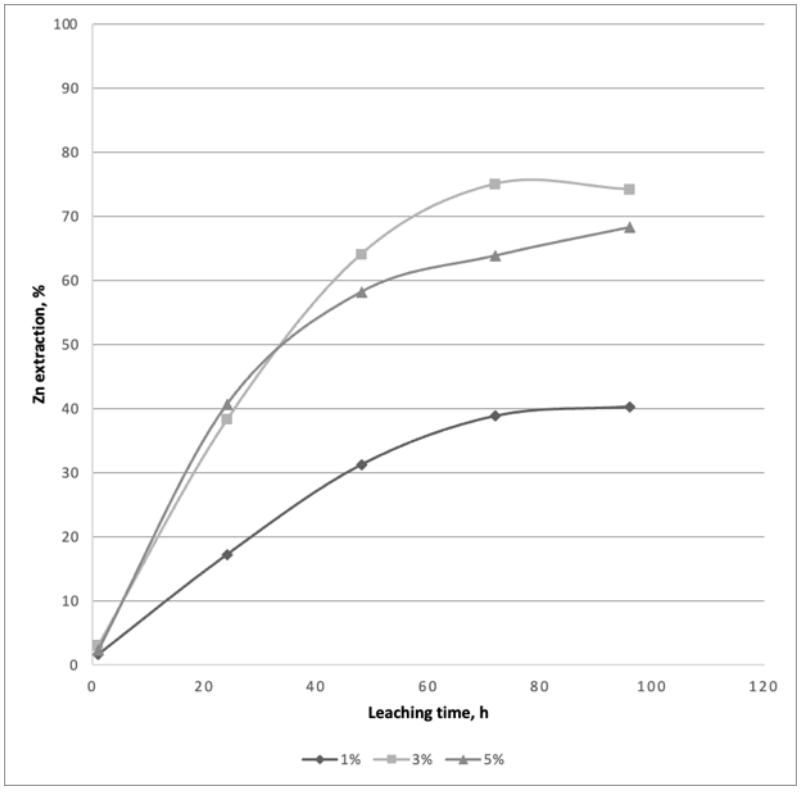

Figure 22. Effect of oxidant on the zinc extraction with 0.5M H_2SO_4 and 5% H_2O_2 at 40°C

4.3 Characterisation of leaching residues

4.3.1 Particle size distribution

The mass retained and the mass passing of residues from various feeds (with varying size fractions) at each screen was noted in Appendix V. The result shows that the P80 of residue from the bulk feed, residue from +50-80 µm feed, and residue from -50 µm feed is 106 µm, 45 µm, and 38 µm, respectively. Table 11 shows the mean particle size (P_{50}) for the leaching feeds with different size fractions and residues.

Table 11. The mean particle size of the feed samples and residue samples

Feed material	Feed, 50% passing	Residue, 50% passing
Bulk	63 µm	53 µm
+50-80 µm	32 µm	32 µm
-50 µm	19 µm	27 µm

It can be observed that the mean particle size for the leaching residue is less than the particle size of the leaching feed in all three samples. It also can be seen that in the bulk sample, which is not milled, the mean particle size has decreased from 63 µm to 53 µm, while the feed with finer particles could be dissolved faster.

4.3.2 Chemical & Mineralogical analysis

In all experiments, leaching residues were characterised using XRD and SEM to understand the solubility behaviour of various zinc phases. XRD was used to identify the phases present in the unleached feed materials and the leaching residues.

In order to detect all the mineral phases in the leach residue, the samples were prepared for XRD analysis. Table 12 summarizes the principal species of the residues detected in the diffractogram at different temperatures (24°C, 40°C, and 60°C); there is a new phase, elemental sulphur. However, it is shown that the temperature does not affect the formation of the new phase.

The result of the residues shows the prominent presence of sphalerite and elemental sulphur. It also claims arsenopyrite, chalcopyrite, pyrite, and quartz in minor amounts and no k-feldspar residue (see Appendix IV). It also shows that the elemental sulphur was detected much lower at room temperature, whereas the elemental sulphur increased at 40°C and 60°C. Moreover, the presence of unreacted sphalerite is also evident. According to the XRD analysis, there is no other variation in the most abundant minerals in the leaching residue. Figure 23 obtained

by SEM showed evidence of a shrinking core model with the formation of elemental sulphur. The formed layer may be porous, non-porous, or, in some cases, detached from the surface. Therefore, the elemental sulphur layer determined the controlling step of the dissolution reaction of zinc or any other metals.

Table 12. Summary of identified minerals using XRD analysis (on different temperatures)

Parameter			Most abundant species	Minority species
Temp	H_2SO_4 concentration, M	H_2O_2 concentration, %		
24°C	0.5	5	Zn(Fe)S and S	FeAsS, $CuFeS_2$, FeS_2, SiO_2
40°C	0.5	5	Zn(Fe)S and S	FeAsS, $CuFeS_2$, FeS_2, SiO_2
60°C	0.5	5	Zn(Fe)S and S	FeAsS, $CuFeS_2$, FeS_2, SiO_2

However, different SEM results showed a high amount of ferrous sulphate in all residues analysed. This can be explained by the chemical reactions taking place; and as a result, ferrous sulphate was formed.

Moreover, the percentage of quartz is shown to be increased due to sphalerite dissolution. The main target elements (Zn, S) of a particle in the leaching residue are illustrated in Figure 23. A well-representative particle was chosen for element maps to show positions of Zn, S, As, Si,

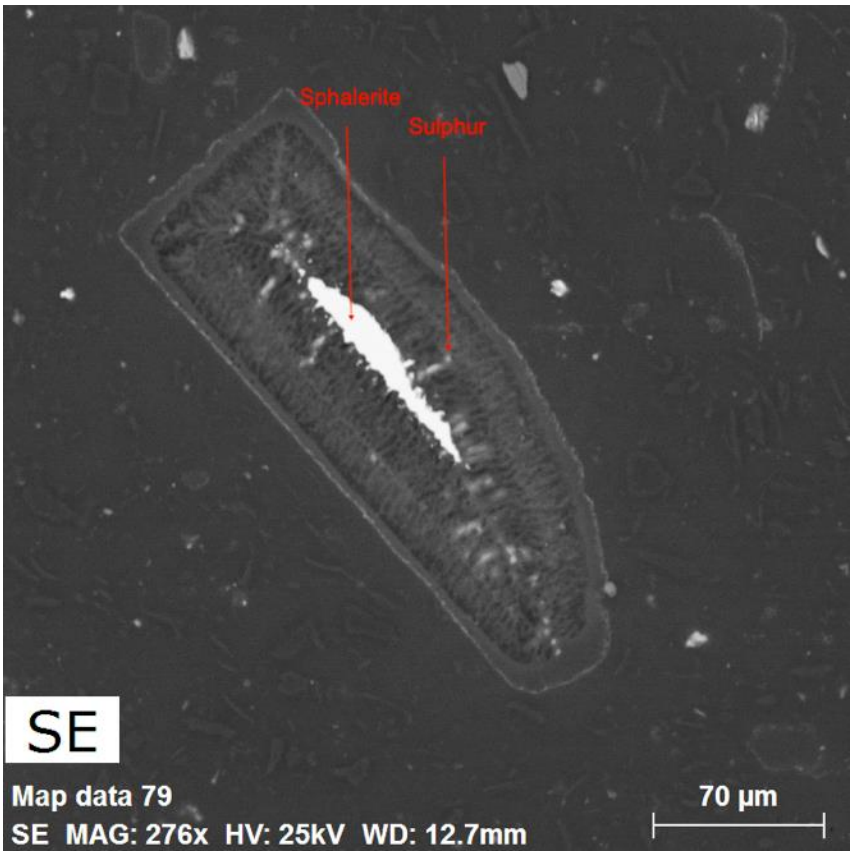

Figure 23. SEM images of leaching residues showing unreacted sphalerite particles surrounded by elemental sulphur

Fe and Cu; there are depicted in Figure 24. Zn is only in the core of the particle, while sulphur surrounds the zinc. It is also worthwhile to mention that higher amount of sulphur is formed as a layer of the sphalerite (see Figure 24b). As and Cu are evenly distributed everywhere, whereas Si is not present in this particle. Finally, sphalerite also bears Fe, and Fe is on the very outer thin layer of the particle (see Figure 24f).

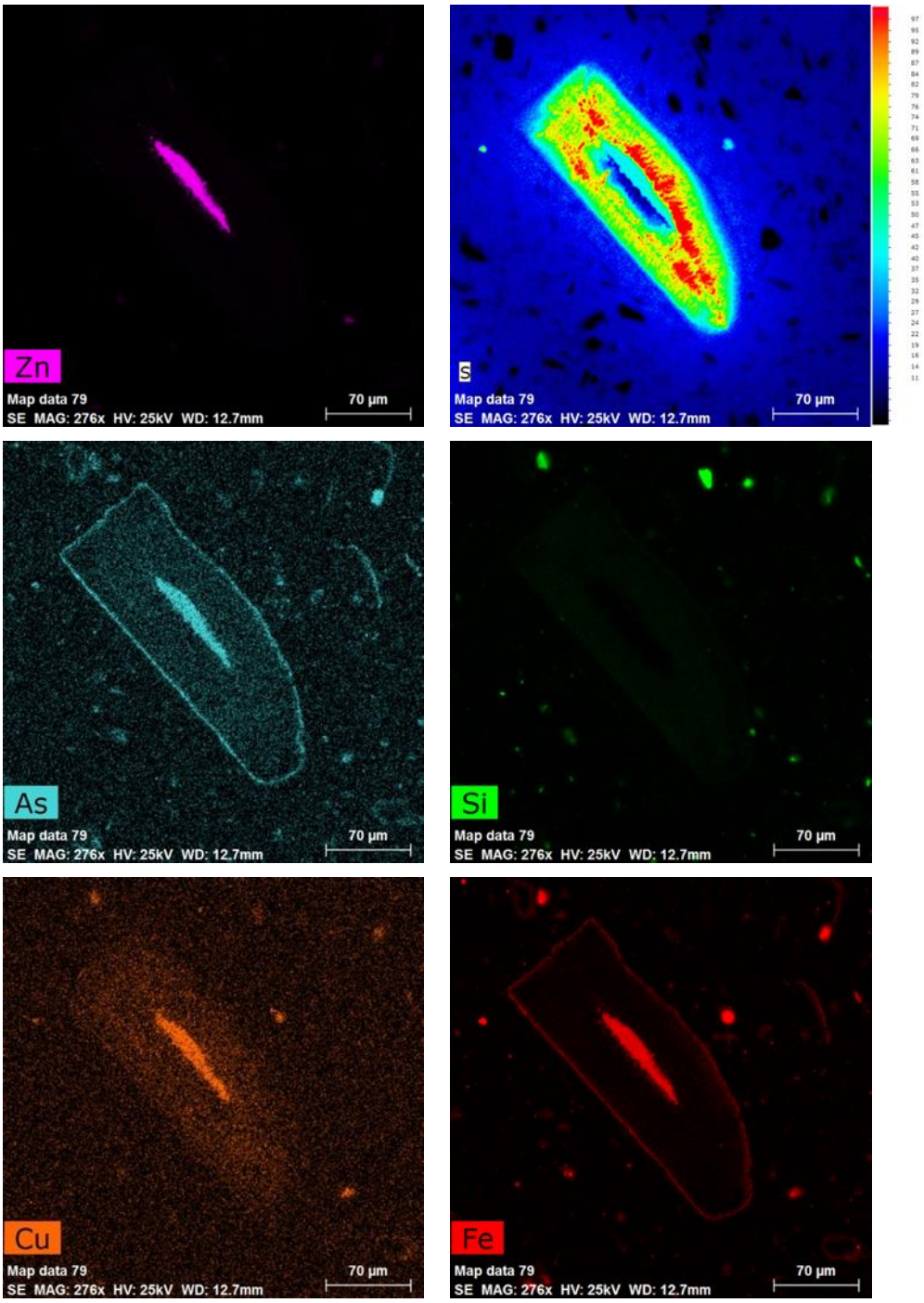

Figure 24. Element maps of the leach residue (Leaching conditions: bulk, 40ºC, 0.5M H_2SO_4 , 5% H_2O_2)

5 Mass Balance

To determine the conditions under which maximum potential recoveries could be achieved, the results from the experiments were used to construct a theoretical mass balance presented in Table 13.

80 g solid dry sample in 800 g solution was considered in the calculation. The feed material was digested using aqua-regia; then, it was leached under the following conditions: at 40°C with 1M H_2SO_4 and 5% H_2O_2 for 96 hours. The residual fraction was recovered by filtration, dried, weighed, and analysed with XRD as described in the Experimental section. The concentrations and total quantities of six metals were considered. The recovery values of the last column were obtained by comparing the quantity of each metal found in the leach and residual fractions. They indicate that the entire metal content of the material is accounted for when using this approach. Only one example is shown, but similar results were obtained for the other samples.

Feed material's chemical composition can be inaccurate due to its incomplete digestion where fluoric acid was not used. Moreover, different analysis techniques cannot be suitable for calculating mass balance as a comparison.

Table 13. Mass balance for leaching process of bulk zinc sulphide

	Feed		Leachate		Residue		Mass balance	
	mg/kg	**µg total**	**mg/kg**	**µg total**	**mg/kg**	**µg total**	**µg total**	**recovery**
Zn	522749,4	41819,9	189574,5	15166,0	522749,4	34151,2	49317,2	1,179
As	18624,1	1489,9	2934,8	234,8	18624,1	1216,7	1451,5	0,974
Cu	15372,6	1229,8	2683,8	214,7	15372,6	1004,3	1219,0	0,991
Fe	149779,9	11982,4	46187,2	3695,0	149779,9	9785,1	13480,1	1,125
Sn	3333,8	266,7	482,7	38,6	3333,8	217,8	256,4	0,961
In	308,7	24,7	105,5	8,4	308,7	20,2	28,6	1,159

6 Economic Feasibility

The technical feasibility and efficiency of the process are one perspective of successfully establishing the procedures. Thus, it is necessary to evaluate the economic reasonability of the processes. The following chapter shows the cost calculation and economic evaluation in every scenario considered. The applied methods are classic financial indicators such as NPV, IRR, and payback period. The economic assessment was conducted based on the operational expenses and capital investment.

In this study, the leaching step and all associated upstream and downstream processes were considered in the calculation. Using LME (London Metal Exchange) zinc price, the potential profit was calculated with an assumed fixed premium. The assumed zinc price and premium were scaled to 100, and all calculations were performed based on this scaling.

6.1 Assumptions

For the economic evaluation, it is essential to address a list of assumptions that had to be made. The detailed version of the individual expenditures and revenues is described in the following sections.

The calculation assumes establishing the processing plant of zinc and indium as a by-product. Fundamental infrastructure like power lines, water pipes, and gas pipelines is presumed to exist on the property. Furthermore, it is assumed that the land required to establish the processing plant is already available, and no other administration buildings need to be built. All legal procedures, official permit costs, and taxes will be considered.

The assumption from the previous study of Irrgang et al. (2021) was taken as-is. Assuming 350000 t of ore mined per year, about 3300 t of tin concentrate, 63000 t of iron concentrate, 52000 t of road gravel, and 17500t of sulphide concentrate could be obtained by processing. The processing of sulphide concentrate is assumed to reach about 40 t per day, which will be used in the planned leaching process, with an annual operation of 334 days per year. This daily quantity of 40 t and 6220 t of metal could be extracted annually. The mass of indium at maximum efficiency would be around 6.6 t per year. Based on the plant's capacity, the dimensions of the required equipment were adjusted. The total cost was estimated based on variable equations, including the dimensions and the capacity, purchase costs, transport of equipment, electric thermal requirements, and energy consumption in the previous studies. As shown in Figure 14, the amortization period and equipment lifetime were assumed to be 20 years. Based on this period, depreciation and annual interest charges were estimated. Additionally, market parameters were defined from the German market.

There are important considerations for a suitable process for the zinc:

- A more favourable economic process is already the case in a leaching system in a sulphuric media with hydrogen peroxide. This implies low operating and capital costs with high zinc recovery
- A low impact on the safety and health of employees and low environmental impact will be preferred.
- The plant will be committed to a low carbon footprint and reducing the use of natural resources. Thus, processes with low energy and water consumption will be preferred.

Different scenarios were investigated to determine the profitability of the different sulphide concentrates.

When considering the calculations, all costs must be estimated in one currency, in this case, the euro. The US dollars to euro value is 1.10 as of March 2021.

Table 14. Basic operating parameters, market parameters, and capitalization parameters (Tran et al., 2020)

Parameters	Values	Units
Basic operating parameters	-	-
Operating period	350	d/a
Processing capacity of a plant	40	t/d
Daily operation period	8	h/d
The factor of safety (for equipment)	20	%
Market parameters		
Annual inflation rate	3	%/a
Annual interest rate	1,8	%/a
Annual discount rate	5,5	%/a
Income tax	30	% of gross income
Exchange rate	1,09	euro/dollar
Capitalization parameters		
Amortization period	20	a
Lifetime of equipment	20	a
Direct costs		
Equipment		
Insulation installation equipment	19	%
Instrumentation and control	3	%
Piping and pipeline systems	7	%
Electrical system	8	%
Building process and services	18	%
Landscaping	3	%
Facilities and services	14	%
Indirect costs		
Engineering and supervision	32	%
Construction spending	10	%
Construction management fees	9	% (direct+indirect cap.)
Contingent fees	26	% (direct+indirect cap.)
Working capital	15	% fixed capital costs

6.2 Process description

6.2.1 Process structure

The bulk sulphide concentrate was produced by processing the pre-treated ore (-1.5mm). In Figure 1, the ore had been ground, sieved, and separated by a spiral concentrator. The following steps include wet ball milling, magnetic separation, gravity separation, hydro cyclones, dewatering, and sulphide flotation (Schach et al., 2019). The final grain size is below 300µm after all the processes mentioned above.

The further processing of the sulphide concentrate can be defined and is presented in Figure 25. Prior to the leaching process, the concentrate must be ground to have a sufficiently small particle size. From the result of the experiments, size reduction accelerates the leaching; thus, such a grinding process enhances the dissolution in the reactor. However, it is vital to find an optimum desired particle size since it requires a tremendous amount of energy from the economic aspect.

In the leaching process, different minerals will be dissolved with the help of sulphuric acid and hydrogen peroxide, which is an oxidising agent, in this case, as described in the lab-scale experiments.

After the leaching, the solution will be thickened, and then the solid will be filtrated.

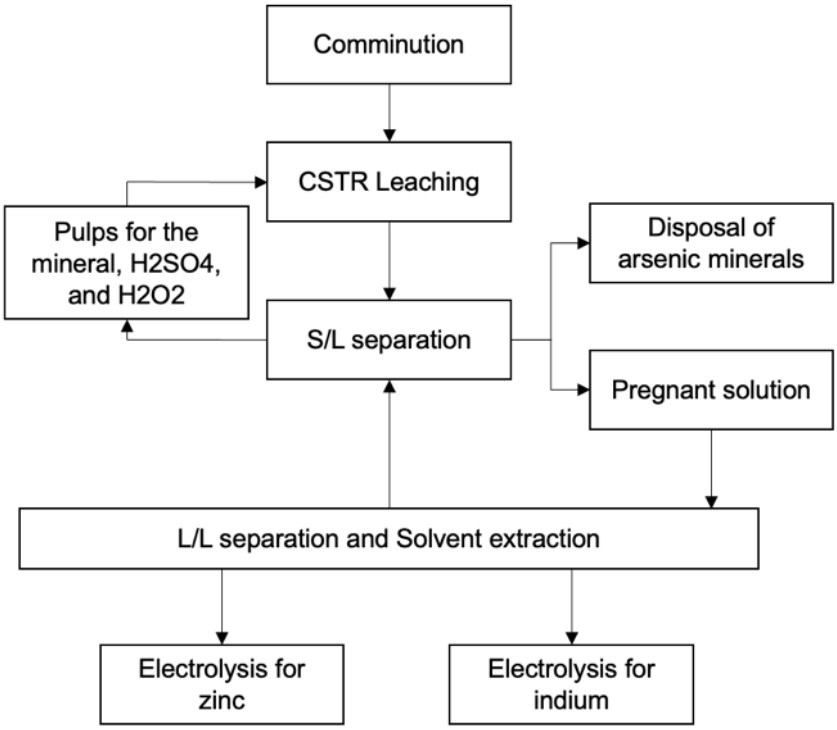

Figure 25. Defined process diagram

6.2.2 Leaching process

Leaching on an industrial scale is mainly carried out in continuously stirred tank reactors (CSTR), which is preferred for processing smaller volumes of valuable material at higher rates.

In order to define process parameters, mineral and chemical characterisations of the leaching material are essential. Once a process with optimal parameters is defined, reactor and agitators can be planned; however, it is a very complex procedure. Additionally, the parameters for the leaching process are chosen in accordance with the mineral's properties.

Leaching parameters are listed in Table 15 based on the results of the leaching process conducted within the scope of the study.

Table 15. Leaching process parameters for calculation of plant size

Temperature, C	40°C
Number of reactors	6
The volume of each reactor	450 m^3
Leaching time, h	48
Grain size	-50 µm
pH value	controlled
Reagents	H_2SO_4, H_2O_2

Economic evaluation is based on the process steps depicted in Figure 25. The calculations considered the leaching step and associated upstream and downstream processes, more precisely the grinding of the bulk sulphide concentrate and the extraction and electrowinning plant. Cost estimates for equipment, namely, agitators, and bead mill, were obtained from Irrgang et al. (2021). Costs for the logistics and construction of buildings as well as other special plant and processing components were determined by conducting online searches of the respective manufacturers. Besides, the costs for conventional solvent extraction, electrowinning plant of the target metals, and dewatering the mixture were derived from the literature.

The maximum leaching extraction of 95% was selected based on the leaching experiments carried out in the laboratory to calculate the required plant size for the solvent extraction and electrowinning section.

Using the assumptions made (see Chapter 6.1) and the result of ICP-OES and XRF analyses of the feed material (see Table 9), the annual zinc production can be calculated as follows:

Capacity[t/yr]=Capacity[t/d]·Operational time[d]· Process extraction

Capacity [t/yr]== 40 t/d · 334 d· 0.95=12692 t/yr

Zinc production[t/yr]=Capacity[t/yr]·Zinc fraction in the feed

Zinc production[t/yr]=12692 t/yr·0.4362=5536 t/yr

Similarly, the annual indium production was calculated, and it was over 876 kg per year.

6.3 Capital Expenditures

All costs are in euros and are converted; variables include working capital, process supplies, and installation. The cost of the pilot-plant equipment is included. Laboratory tests, which were performed in this study, can be helpful in determining which alternative is preferable.

All equipment was listed, and equipment costs of milling, leaching, logistics, and buildings were taken from the study of Irrgang et al. (2021) since the whole processes are similar, while costs of extraction electrowinning were taken from other literature (Sinclair, 2005; Tran et al., 2020).

Generally, Capital expenditures are classified as direct and indirect costs. Direct costs are expenses incurred during the production of a good or service and may be variable costs, fluctuating according to the number of goods and services. In this case, direct costs are for plant components. The cost estimate includes 6 reactors to achieve the 48h residence time. The reactors can be designed based on the technical specifications required. Thus, the actual cost is not available in the open domain. However, indirect costs are for the construction and planning or administrative expenses, which we cannot assign to specific objects. In this study, indirect costs represented 15% of total direct costs and were added to total CAPEX (Sinclair, 2005).

The extraction and electrowinning process varies depending on the metal; thus, different electrowinning plants are required for specific metals. The cost and volume of components used in leaching, extraction, and electrowinning facilities are proportional to the amount of concentrate to be processed. As a result, the cost of solvent extraction with related equipment was estimated at a unit of $ per tonne, which is annually produced of metals of interest.

CAPEX can fluctuate at different rates based on the financial method and payback time. Comparing CAPEX to operating costs, it is much easier to plant and estimate because there are many common such plants in real life. Generally, costs alter due to a few suppliers; and its planning is unreliable.

Table 16. Capital costs for plants and equipment

Equipment	Purpose and Specifications	Unit cost, €	Quantity	Total cost, €	% of direct costs	Reference
Agitator bead mill	For milling; 40t/d, 300 µm to 45 µm	257075	2	514.150	2.03	(Irrgang et al., 2021; Tran et al., 2020)
Reactors	For leaching, 450 m^3, steel, with a stirrer	154245	6	9.254.700	36.57	
Others	Sensors; cooling systems; external fans		Sensors-6 Cooling equipment-8 Fans - 13	1.209.481	4.78	
Buildings	Plants of leaching, extraction, and electrowinning; buildings for administration, personnel, lab	1419200	2	2.838.400	11.22	(Tran et al., 2020)
Transport	Forklifts	55055	6	330.330	1.31	
Conveyor system	30 m			136.500	0.54	
Electricity distribution				228.500	0.90	
Extraction plant	Separation of solid/liquid and liquid/liquid	3401850	1	3.401.850	13.44	(Sinclair, 2005; Tran et al., 2020)
Electrowinning plant	Zinc/Indium	7393950	1	7.393.950	29.22	
Total direct cost				**25.307.861**	100	
Indirect costs	Planning and execution			**3.796.180**	15	
Total costs				**29.104.040**		

6.4 Operational expenditures

All operating costs per unit are presented in Figure 17. Operational expenses consist of variable and fixed costs. The fixed operating costs include fees for labour, maintenance, insurance, land rental, property taxes, and administrative costs. Over 55% of the total operating cost goes to fixed costs (Fuls & Petersen, 2013).

The variable costs of the leaching depend on factors such as the concentration of and the price of the reagents used and the electricity and water consumption. A large amount of the electric power would be consumed by continuous stirring with agitators. The larger the reactor, the larger the drive power is required. Heating and cooling of the solution, pumps, control and measuring instruments, IT requirements, and even primary consumers such as lighting and ventilation would contribute to electricity consumption. Since the electricity price is relatively in Germany, there are some complex procedures to calculate energy cost. Irrgang et al. (2021) used the average unit price of electricity as 0.19 €/kWh. After usage of 1GWh, the price will be reduced to 0.1202 €/kWh as stated in the energy tax levels in Germany.

Besides the energy consumption, the reagents, especially H_2O_2, are consumed in this leaching process, resulting in more costs in operation. The reagent cost estimate is based on consumption rates presented and recent quotations from suppliers; thus, no material balance is done for the reagents used in this section. Generally, the bulk concentrate requires a large amount of solvent. From an economic point of view, the solvent must be cheap and regenerative. However, the cost of reagents for leaching in a small bulk is not an essential factor.

Due to lower maintenance costs, direct atmospheric leaching is less expensive than direct pressure leaching (Picazo-Rodríguez et al., 2020). The maintenance cost is expected components and brick lining are not needed for the atmospheric reactors. Hence, the maintenance cost is 2% of the final CAPEX, while the depreciation is estimated at 10t.

OPEX is sensitive to the process chemistry involving redox potential, pH of leaching stages, and the precipitation of iron during the leaching. This leaching process has achieved high zinc recovery with the help of feed material size distribution; thus, particle size distribution is required based on the mineralogy and kinetics. Moreover, sulphuric acid consumption for this process is two times more than the acid consumption of the acid pressure leaching process (Fuls & Petersen, 2013).

Table 17. Operation costs for plants

Parameters	Description	Value	Units	Cost/yr	Cost/ t metal	References
Direct operating costs						
Chemicals						
H_2SO_4, 98%	Industrial sulphuric acid	10	%/total OPEX	740,854	133	(Tran et al., 2020)
H_2O_2	Industrial H_2O_2	10	%/total OPEX	740,854	133	
Labor						
Unit cost for personnel	25 units	45000	€/yr	1,125,000	203	(Irrgang et al., 2021)
Utilities						
Unit cost for electricity	33371318kWh/yr	0.19/0.1202	€/kWh	4,081,032	737	
Unit cost for water consumption	86700 m^3/yr	1.60	€/m^3	138,720	25	
Maintenance and repair		2	% capital costs /yr	582,081	105	
Total				**7,408,541**	**1336**	

6.5 Financial indicators

6.5.1 Cash flow calculation

The cash flow calculation refers to money movement in and out of the enterprise. Since the metal dissolution rate of 95% was selected for leaching based on the laboratory experiment results. Furthermore, the efficiency of the extraction and electrowinning process was not included in the cash flow calculation. The average price of the last 5 years concerning the quality of 99,99% as a product on the market for zinc price. For indium, setting a price is complicated due to its high fluctuation since China supplies indium demand predominantly worldwide; thus, the calculation of indium price will be considered the latest possible date. The average price of zinc between 2017 and 2022 was approximately 2502 €/t (Zinc - 2022 Data,

n.d.), whereas the average indium price was 207.85 €/kg as of 2022 (Indium-Germanium-Gallium Price Chart, n.d.).

The annual revenues of the sale of zinc and indium were calculated using the equation above and displayed in Table 18.

Table 18. Calculation of revenue from sales of metal

Metal	Production, t/yr	Price,€/t	Revenue, €/yr
Zn	5536.63	2502.5	13855419.48
In	0.876	207850	182024.2218
Total	5537.51		14037443.70

6.5.2 NPV & IRR calculations

Essential indicators in investment decisions such as net present value (NPV) and internal rate of return (IRR) were calculated based on the average market price of zinc and indium in different scenarios. The NPV is widely applied for budgeting capital and allows investors to see if a project is profitable. The IRR is a metric used in financial analysis to estimate the profitability of potential investments and decide the use of cash during budget planning.

A simple NPV calculation was performed when the production period and the discount rate were set to 20 years and 10%, respectively, since the investment is high risk. The calculation result is shown in Table 19; the progress of the NPV each year can be observed and shown in Figure 26. Due to the initial investments, the NPV is negative in the first years of the operation and increases the lifetime. At the end of the project's lifetime, the beneficiation plant can be profitable within the project period since the NPV is around 20,41 million euros. It is important to note that NPV analysis involves cash flows before tax because of the different tax laws and

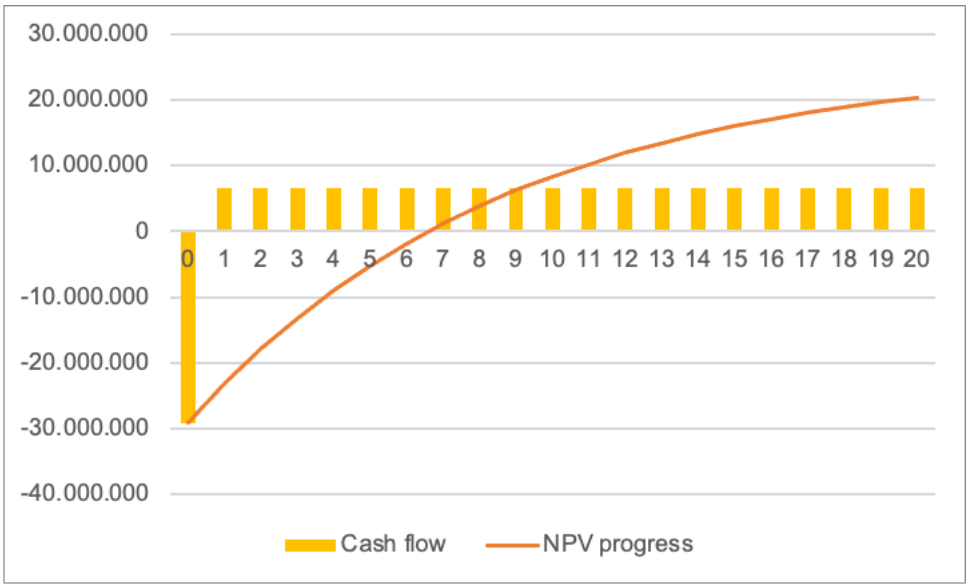

Figure 26. NPV progress of the proposed beneficiation plant with 10% discount rate

regulations for depreciation of investments and investment costs in different countries. The internal discount rate, which depends on trends in the global economy, significantly affects the NPV change.

Table 19. Data needed for the calculation & results of NPV and IRR

Lifetime	20 years
Discount rate	12%
Initial investment =CAPEX	29.104.040 €
Revenue per a year	14037443,70 €
OPEX	7,408,541€
Profit	6628902,7€
NPV	**20.410.175€**
IRR	**9,26%**

7 Conclusions & Recommendations

This thesis focuses on extracting zinc and the possibility of the indium as by- production from the sulphide concentrate, which was previously processed in the Tellerhäuser pilot plant, by direct acid leaching process with sulphuric acid and hydrogen peroxide as reagents.

As the overview of the experimental results, key parameters affecting the leaching efficiency such as temperature, acid concentration, particle size, and oxidant concentration were studied. Although different pulp densities and other oxidising agents could not be studied in this study and would be a part of future investigations. Leaching tests with higher temperatures than the room temperature resulted in higher metal extraction. However, due to the hydrogen peroxide's high sensitivity to the temperature set, the optimum temperature is 40°C in the subsequent experiments. Different sulphuric acid concentrations resulted in other effects on the various metal extractions due to changes in pH during the leaching process. The results show that As, Fe, and In had similar leaching behaviours, which may be advantageous for further procedures such as solvent extraction to separate gangue metals from the solution by selectively precipitation. The overall trend of the zinc extraction was that the extraction percentage increased as the acid concentration increased. Next, the size fraction is crucial in the leaching process and economic profitability in reducing the operational expenditure of energy consumption. Finding an optimum size fraction can lead to adequate milling time. In addition to adding hydrogen peroxide, pumping hydrogen peroxide slowly showed much better results on the metal extractions; however, further experiments or studies must be conducted to improve the leaching kinetics and leaching time. Besides, it was also essential to keep the storage condition of hydrogen peroxide during the leaching.

The highest zinc extraction was achieved when -50 µm of particle size feed material with 1.5M sulphuric acid and 5% hydrogen peroxide at 40°C. The result indicates that strong and expensive oxidising agents to achieve high leaching yields of this complex sulphide concentrate are inevitable.

For the theoretical mass balance, several results of different analyses such as XRD and ICP-OES were used; there were small deviations explained by different types of data from various analysing techniques; therefore, it should be noted in future studies. Other experimental design techniques are recommended for similar studies to decrease the number of experiments. To maintain a constant pH in the system, an acidic solution must be added. However, it must be noted that the S/L ratio must remain constant. ANOVA analysis of the parameters for zinc extraction will identify the essential factors for the leaching, reducing the number of experiments required.

The leaching solution contained a high percentage of copper and iron because of the solubility of these elements in the utilised sulphate medium with the given temperature and acid concentration. It is essential to consider that the solution could be treated in solvent extraction and electrowinning stages to produce electrolytic zinc. The raffinate from solvent extraction could be neutralised with calcium carbonate to precipitate ferric ions, copper, arsenic, and minor elements. The solution could be recycled to the direct leaching stage (Cháidez et al., 2019).

The acid concentration must be considered a critical parameter from an economic perspective. An excess of sulphuric acid will increase the neutralising agent in the posterior stages of the leaching process. In contrast, a lack of sulphuric acid could result in the precipitation of iron, creating difficulties in the recovery of valuable metals at later stages.

Despite the economic and environmental advantages of direct leaching, the development of the direct leaching approach still requires further research because of the formation of sulphur passivation layer challenges. The passivation layer precipitates on the sphalerite surface, hindering further leaching; hence a fraction of the sulphide mineral is left.

A more precise conception and calculation of the reactor size is only possible with further experiments in pilot plants. With the help of additional tests, it can be assessed whether the planned volume of the reactors can be further reduced, thus reducing investment costs. A reduction in volume can be achieved through a higher proportion of solids in the leaching mixture.

By analysing the state of the art of direct atmosphere acid leaching technologies, a potential set-up of the operation was developed based on laboratory-scale experiments considering a sufficient economic project structure. In practice, various geological conditions and local constraints, and differences in cost estimations may yield a negative economic result for this plant. However, geological, technical, and economic parameters can be distinguished to enable an economically feasible operation. In this study, the project can be viable for a defined case. However, further detailed analyses such as sensitivity and risk analysis must be performed to determine the most parameters contributing to economic feasibility.

Moreover, the environmental aspects of such processing methods are a significant issue. Even though the direct acid leaching process produces elemental sulphur instead of sulphur dioxide and other harmful gases, it requires a particular storage area. Besides, a minor amount of arsenic can hinder further usage of the sulphur residue without purification.

Bibliography

- *Zi*nc metal consumption 2020 | Statista. (n.d.). Retrieved February 12, 2022, from https://www.statista.com/statistics/264884/world-zinc-usage/

Anderson, C. G., Dunne, R. C., & Uhrie, J. L. (2014). Mineral processing and extractive *metallurgy : 100 years of i*nnovation (C. G. Anderson, R. C. Dunne, & J. L. Uhrie, Eds.) [Book]. Published by Society for Mining, Metallurgy & Exploration Inc.

Antonijević, M. M., Dimitrijević, M., & Janković, Z. (1997). Leaching of pyrite with hydrogen peroxide in sulphuric acid. Hydrometallurgy, 46(1–2), 71–83. https://doi.org/10.1016/S0304-386X(96)00096-5

Asadi Zeydabadi, B., Mowla, D., Shariat, M. H., & Fathi Kalajahi, J. (1997). Zinc recovery from blast furnace flue dust. Hydrometallurgy, 47(1), 113–125. https://doi.org/10.1016/S0304-386X(97)00039-X

Aydogan, S. (2006). Dissolution kinetics of sphalerite with hydrogen peroxide in sulphuric acid medium. Chemical Engineering Journal, 123(3), 65–70. https://doi.org/10.1016/J.CEJ.2006.07.001

Babu, M. N., Sahu, K. K., & Pandey, B. D. (2002). Zinc recovery from sphalerite concentrate by direct oxidative leaching with ammonium, sodium and potassium persulphates. Hydrometallurgy, 64(2), 119–129. https://doi.org/10.1016/S0304-386X(02)00030-0

Balarini, J. C., Polli, L. de O., Miranda, T. L. S., Castro, R. M. Z. de, & Salum, A. (2008). Importance of roasted sulphide concentrates characterization in the hydrometallurgical extraction of zinc. Minerals Engineering, 21(1), 100–110. https://doi.org/10.1016/J.MINENG.2007.10.002

Barakat, M. A. (2003). The pyrometallurgical processing of galvanizing zinc ash and flue dust. JOM 2003 55:8, 55(8), 26–29. https://doi.org/10.1007/S11837-003-0100-4

Cháidez, J., Parga, J., Valenzuela, J., Carrillo, R., & Almaguer, I. (2019). Leaching Chalcopyrite Concentrate with Oxygen and Sulfuric Acid Using a Low-Pressure Reactor. Metals 2019, Vol. 9, Page 189, 9(2), 189. https://doi.org/10.3390/MET9020189

Constantineau, J. P., & Eng, B. (2004). *Fluidized bed roasting of zinc sulfide concentrate :* factors affecting the particle size distribution. https://doi.org/10.14288/1.0058659

Dimitrov, R. I., Moldovanska, N., Bonev, I. K., & Živkovic, Ž. (2000). Oxidation of marmatite. Thermochimica Acta, 362(1–2), 145–151. https://doi.org/10.1016/S0040-6031(00)00582-7

Dutrizac, J. E. (John E.). (n.d.). Lead-*Zinc 2000 : proceedings of the Lead*-Zinc 2000 Symposium which was part of the TMS Fall Extraction & Process Metallurgy Meeting, Pittsburgh, U.S.A., October 22-25, 2000. 960.

Filippou, D. (2004). Innovative hydrometalurgical processes for the primary processing of zinc. Mineral Processing and Extractive Metallurgy Review, 25(3), 205–252. https://doi.org/10.1080/08827500490441341

Filippou, D. (2010). INNOVATIVE HYDROMETALLURGICAL PROCESSES FOR THE PRIMARY PROCESSING OF ZINC. Http://Dx.Doi.Org/10.1080/08827500490441341, 25(3), 205–252. https://doi.org/10.1080/08827500490441341

Forero-Saboya, J., Davoisne, C., Dedryvère, R., Yousef, I., Canepa, P., & Ponrouch, A. (2020). Understanding the nature of the passivation layer enabling reversible calcium plating. Energy & Environmental Science, 13(10), 3423–3431. https://doi.org/10.1039/D0EE02347G

Frenzel, M., Mikolajczak, C., Reuter, M. A., & Gutzmer, J. (2017). Quantifying the relative availability of high-tech by-product metals – The cases of gallium, germanium and indium. Resources Policy, 52, 327–335. https://doi.org/10.1016/J.RESOURPOL.2017.04.008

Fuls, H. F., & Petersen, J. (2013). Evaluation of processing options for the treatment of zinc sulphide concentrates at Skorpion Zinc. Journal of the Southern African Institute of Mining and Metallurgy, 113(5). http://www.scielo.org.za/scielo.php?script=sci_arttext&pid=S2225-62532013000500008

Ghassa, S., Noaparast, M., Shafaei, S. Z., Abdollahi, H., Gharabaghi, M., & Boruomand, Z. (2017). A study on the zinc sulfide dissolution kinetics with biological and chemical ferric reagents. Hydrometallurgy, 171, 362–373. https://doi.org/10.1016/J.HYDROMET.2017.06.012

Ghayad, I. M., El-Ansary, A. L., Hamid, Z. A., & El-Akshr, A. A. (2019). Recovery of Zinc from Zinc Dross Using Pyrometallurgical and Electrochemical Methods. Egyptian Journal of Chemistry, 62(2), 373–384. https://doi.org/10.21608/EJCHEM.2018.2782.1225

Gu, Y., Zhang, T. A., Liu, Y., Mu, W. Z., Zhang, W. G., Dou, Z. H., & Jiang, X. L. (2010). Pressure acid leaching of zinc sulfide concentrate. Transactions of Nonferrous Metals Society of China, 20(SUPPL.1), s136–s140. https://doi.org/10.1016/S1003-6326(10)60028-3

Habashi, F. (1997). Handbook of Extractive Metallurgy, Volume 2. In Fathi Habashi (Vol. 2). https://www.academia.edu/292081/Handbook_of_Extractive_Metallurgy_Volume_2

Hackl, R. P., Dreisinger, D. B., Peters, E., & King, J. A. (1995). Passivation of chalcopyrite during oxidative leaching in sulfate media. Hydrometallurgy, 39(1–3), 25–48. https://doi.org/10.1016/0304-386X(95)00023-A

Helbig, T., Gilbricht, S., Lehmann, F., Daus, B., Kelly, N., Haseneder, R., & Scharf, C. (2018). Oxidative leaching of a sulfidic flue dust of former copper shale processing with focus on rhenium. Minerals Engineering, 128, 168–178. https://doi.org/10.1016/J.MINENG.2018.08.028

Hilgers, C., & Becker, I. (2020). Local availability of raw materials and increasing global demand – aspects of resilient resource strategies = Lokale Verfügbarkeit von Rohstoffen bei steigender globaler Nachfrage – Aspekte zu resilienten Ressourcenstrategien. World of mining, surface & underground, 72(5), 254–263.

Irrgang, N., Monneron-Enaud, B., Möckel, R., Schlömann, M., & Höck, M. (2021). Economic feasibility of the co-production of indium from zinc sulphide using bioleaching extraction in Germany. Hydrometallurgy, 200, 105566. https://doi.org/10.1016/J.HYDROMET.2021.105566

Ke, Y., Chai, L. Y., Min, X. B., Tang, C. J., Chen, J., Wang, Y., & Liang, Y. J. (2014). Sulfidation of heavy-metal-containing neutralization sludge using zinc leaching residue as the sulfur source for metal recovery and stabilization. Minerals Engineering, 61, 105–112. https://doi.org/10.1016/J.MINENG.2014.03.022

Kim, B.-S., Jeong, S.-B., Kim, Y., & Kim, H.-S. (2010). Oxidative Roasting of Low Grade Zinc Sulfide Concentrate from Gagok Mine in Korea. MATERIALS TRANSACTIONS, 51(8). https://doi.org/10.2320/matertrans.M2010045

Lalancette, J.-M., Dubreuil, B., & Lemieux, D. (2012). Method for selective precipitation of iron, arsenic and antimony.

Mahajan, V., Misra, M., Zhong, K., & Fuerstenau, M. C. (2007). Enhanced leaching of copper from chalcopyrite in hydrogen peroxide–glycol system. Minerals Engineering, 20(7), 670–674. https://doi.org/10.1016/J.MINENG.2006.12.016

Metz, S., & Trefry, J. H. (2000). Chemical and mineralogical influences on concentrations of trace metals in hydrothermal fluids. Geochimica et Cosmochimica Acta, 64(13), 2267–2279. https://doi.org/10.1016/S0016-7037(00)00354-9

Mubarok, M. Z., Sukamto, K., Ichlas, Z. T., & Sugiarto, A. T. (2018). Direct sulfuric acid leaching of zinc sulfide concentrate using ozone as oxidant under atmospheric pressure. Minerals & Metallurgical Processing 2018 35:3, 35(3), 133–140. https://doi.org/10.19150/MMP.8462

Nicol, M. J. (2020). The role and use of hydrogen peroxide as an oxidant in the leaching of minerals. 1. acid solutions. Hydrometallurgy, 193, 105328. https://doi.org/10.1016/J.HYDROMET.2020.105328

Ozberk, E., Jankola, W. A., Vecchiarelli, M., & Krysa, B. D. (1995). Commercial operations of the Sherritt zinc pressure leach process. Hydrometallurgy, 39(1–3), 49–52. https://doi.org/10.1016/0304-386X(95)00047-K

Pecina, T., Franco, T., Castillo, P., & Orrantia, E. (2008). Leaching of a zinc concentrate in H2SO4 solutions containing H2O2 and complexing agents. Minerals Engineering, 21(1), 23–30. https://doi.org/https://doi.org/10.1016/j.mineng.2007.07.006

Picazo-Rodríguez, N. G., Soria-Aguilar, M. D. J., Martínez-Luévanos, A., Almaguer-Guzmán, I., Chaidez-Félix, J., & Carrillo-Pedroza, F. R. (2020). Direct Acid Leaching of Sphalerite:

An Approach Comparative and Kinetics Analysis. Minerals 2020, Vol. 10, Page 359, 10(4), 359. https://doi.org/10.3390/MIN10040359

Rabah, M. A., & El-Sayed, A. S. (1995). Recovery of zinc and some of its valuable salts from secondary resources and wastes. Hydrometallurgy, 37(1), 23–32. https://doi.org/10.1016/0304-386X(94)00015-U

Ramachandran, P., Nandakumar, V., & Sathaiyan, N. (2004). Electrolytic recovery of zinc from zinc ash using a catalytic anode. Journal of Chemical Technology & Biotechnology, 79(6), 578–583. https://doi.org/10.1002/JCTB.1007

Sadeghi, N., Moghaddam, J., & Ilkhchi, M. O. jaghi. (2016). Determination of effective parameters in pilot plant scale direct leaching of a zinc sulfide concentrate. Physicochemical Problems of Mineral Processing, 53(1), 601–616. https://doi.org/10.5277/PPMP170147

Safari, V., Arzpeyma, G., Rashchi, F., & Mostoufi, N. (2009). A shrinking particle—shrinking core model for leaching of a zinc ore containing silica. International Journal of Mineral Processing, 93(1), 79–83. https://doi.org/10.1016/J.MINPRO.2009.06.003

Sahu, S. K., Sahu, K. K., & Pandey, B. D. (2006). Leaching of zinc sulfide concentrate from the ganesh-himal deposit of nepal. Metallurgical and Materials Transactions B, 37(4). https://doi.org/10.1007/s11663-006-0037-4

Santos, S. M. C., Machado, R. M., Correia, M. J. N., Reis, M. T. A., Ismael, M. R. C., & Carvalho, J. M. R. (2010). Ferric sulphate/chloride leaching of zinc and minor elements from a sphalerite concentrate. Minerals Engineering, 23(8), 606–615. https://doi.org/10.1016/J.MINENG.2010.02.005

Schach, E., Padula, F., Buchmann, M., Möckel, R., Ebert, D., Pereira, L., Kern, M., Leißner, T., Pashkevich, D., Sousa, R., Bremerstein, I., Breuer, B., Oliver, K., Seltmann, R., Reimer, W., Wotruba, H., Filippov, L., Peuker, U., Rudolph, M., … van den Boogaart, K. G. (2021). Data from a pilot plant experiment for the processing of a complex tin skarn ore - 19.11.2018. https://doi.org/10.14278/RODARE.715

Schach, E., Pereira, L., Padula, F., Möckel, R., Ebert, D., Buchmann, M., Leißner, T., Pashkevich, D., Sousa, R., Kern, M., Bremerstein, I., Filippov, L., Rudolph, M., Broadbent, C., Roscher, M., & Boogart, K. (2019). Pilot Plant for the Processing of a Complex Tin Ore: a Contribution towards Geometallurgy in Beneficiation. https://doi.org/10.13140/RG.2.2.27346.50883

Schuppan, Werner., Hiller, Axel., & Krejny, Inge. (2012). Die Komplexlagerstätten Tellerhäuser *und Hämmerlein : Uranbergbau und Zinnerkundung* in der Grube Pöhla der SDAG Wismut. https://books.google.com/books/about/Die_Komplexlagerst%C3%A4tten_Tellerh%C3%A4user_u.html?hl=de&id=YTytlwEACAAJ

Shamsuddin, M. (2021a). Hydrometallurgy. Minerals, Metals and Materials Series, 429–529. https://doi.org/10.1007/978-3-030-58069-8_11

Shamsuddin, M. (2021b). Roasting of Sulfide Minerals. Minerals, Metals and Materials Series, 39–68. https://doi.org/10.1007/978-3-030-58069-8_2

Silin, I., Hahn, K. M., Gürsel, D., Kremer, D., Gronen, L., Stopić, S., Friedrich, B., & Wotruba, H. (2020). Mineral Processing and Metallurgical Treatment of Lead Vanadate Ores. Minerals 2020, Vol. 10, Page 197, 10(2), 197. https://doi.org/10.3390/MIN10020197

Simons, B., Andersen, J. C., Rollinson, G., Armstrong, R., Dolgopolova, A., Seltmann, R., Stanley, C., Roscher, M., Simons, B., Andersen, J. C., Rollinson, G., Armstrong, R., Dolgopolova, A., Seltmann, R., Stanley, C., & Roscher, M. (2017). Mineralogical variation of skarn ore from the Tellerhäuser deposit, Pöhla, Germany. EGUGA, 19, 8577. https://ui.adsabs.harvard.edu/abs/2017EGUGA..19.8577S/abstract

Sinclair, R. J. (2005). The Extractive Metallurgy of Zinc (1st ed., Vol. 13). The Australasian Institute of Mining and Metallurgy .

SMFE. (n.d.). Indium-Germanium-Gallium Price Chart. Retrieved March 28, 2022, from https://price.metal.com/Indium-Germanium-Gallium

Takacova, Z., & Trpčevská, J. (2010). Leaching of zinc from zinc ash originating from hot-dip galvanizing Hard zinc processing, production of alloys from zinc drosses View project. https://www.researchgate.net/publication/287009706

Thorsen, G., Grislingas, A., & Steintveit, G. (2014). Recovery of Zinc from Zinc Ash and Flue Dusts by Hydrometallurgical Processing. JOM 1981 33:1, 33(1), 24–29. https://doi.org/10.1007/BF03354397

Tran, L. H., Tanong, K., Jabir, A. D., Mercier, G., & Blais, J. F. (2020). Hydrometallurgical Process and Economic Evaluation for Recovery of Zinc and Manganese from Spent Alkaline Batteries. Metals 2020, Vol. 10, Page 1175, 10(9), 1175. https://doi.org/10.3390/MET10091175

Treliver Minerals Ltd. (2015, March 19). Treliver reports new Tellerhäuser resource - International Tin Association. https://www.internationaltin.org/treliver-reports-new-tellerhauser-resource/

Trpčevská, J., Hǫková, B., Briančin, J., Korálová, K., & Pirošková, J. (2015). The pyrometallurgical recovery of zinc from the coarse-grained fraction of zinc ash by centrifugal force. International Journal of Mineral Processing, 143, 25–33. https://doi.org/10.1016/J.MINPRO.2015.08.006

Turan, M. D., Altundoğan, H. S., & Tümen, F. (2004). Recovery of zinc and lead from zinc plant residue. Hydrometallurgy, 75(1–4), 169–176. https://doi.org/10.1016/J.HYDROMET.2004.07.008

Wang, Z., Gao, J., Shi, A., Meng, L., & Guo, Z. (2018). Recovery of zinc from galvanizing dross by a method of super-gravity separation. Journal of Alloys and Compounds, 735, 1997–2006. https://doi.org/10.1016/J.JALLCOM.2017.11.385

Xie, K. qiang, Yang, X. wan, Wang, J. kun, Yan, J. feng, & Shen, Q. feng. (2007). Kinetic study on pressure leaching of high iron sphalerite concentrate. Transactions of Nonferrous Metals Society of China, 17(1), 187–194. https://doi.org/10.1016/S1003-6326(07)60070-3

Ylä-Mella, J., & Pongrácz, E. (2016). Drivers and Constraints of Critical Materials Recycling: The Case of Indium. Resources 2016, Vol. 5, Page 34, 5(4), 34. https://doi.org/10.3390/RESOURCES5040034

Zinc - 2022 Data. (n.d.). Retrieved March 28, 2022, from https://tradingeconomics.com/commodity/zinc

List of Appendixes

Appendix I. Material splitting procedure

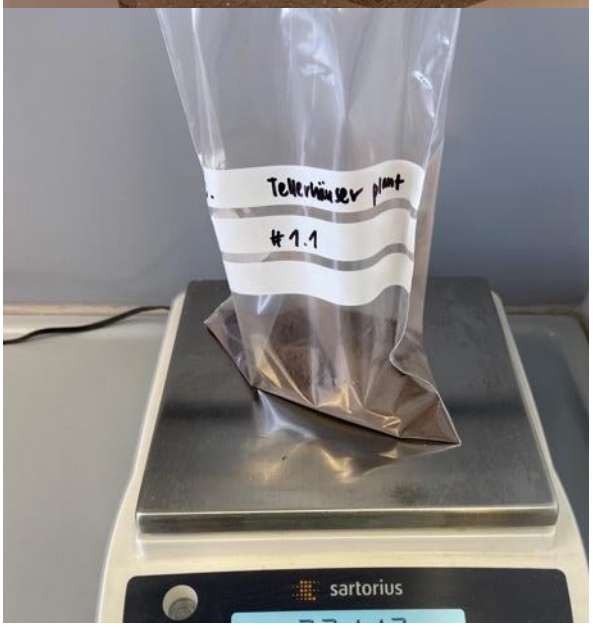

Appendix II. Particle size distribution of materials with different milling time

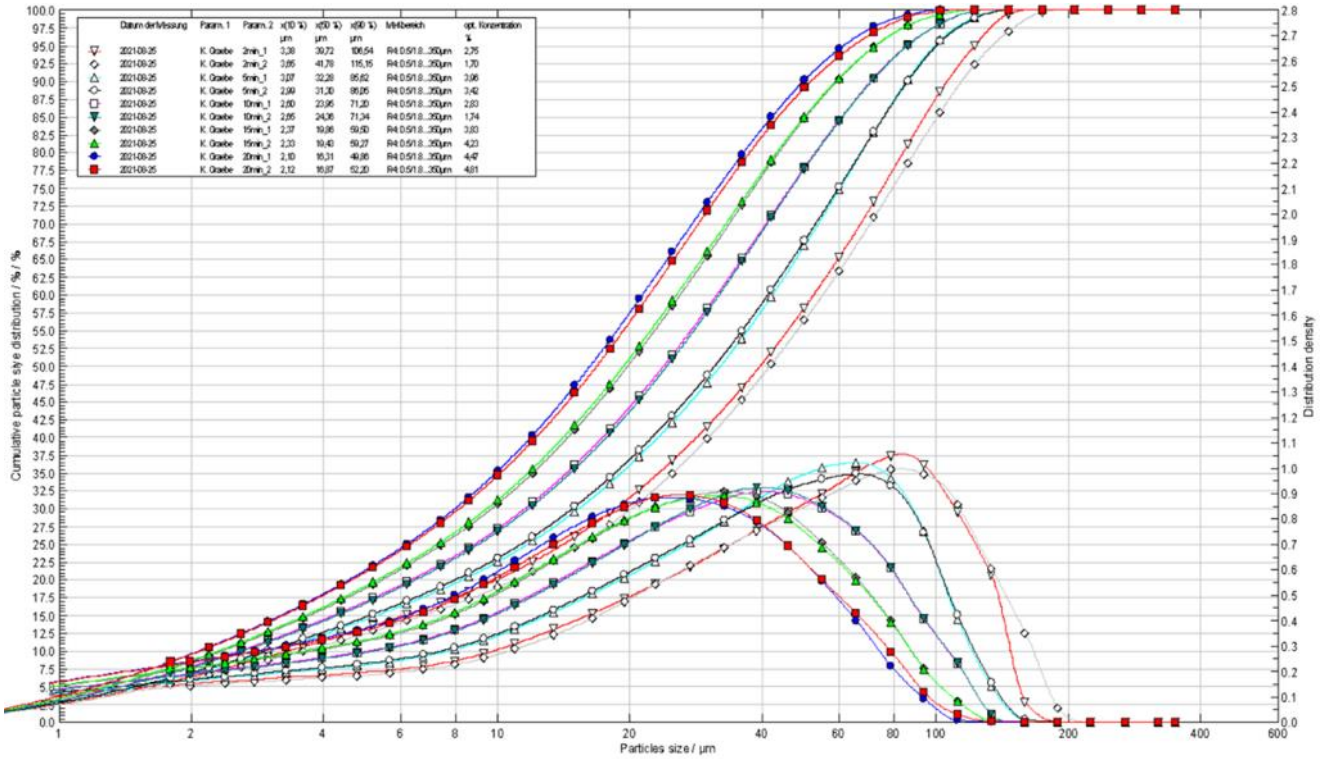

Appendix III. Chemical composition data (by MLA)

Table 20. Chemical Assay of feed by MLA

Element	Bulk	+50-80 µm	-50 µm
Al	0,66	0,62	0,77
As	1,34	1,70	1,80
C	0,03	0,03	0,03
Ca	1,32	1,27	1,52
Ce	0,00	0,00	0,00
Cl	0,07	0,07	0,09
Cr	0,01	0,01	0,01
Cu	1,07	1,23	1,33
F	0,21	0,21	0,28
Fe	15,13	15,47	16,07
Gd	0,00	0,00	0,00
H	0,02	0,02	0,02
K	0,20	0,20	0,24
La	0,00	0,00	0,00
Li	0,00	0,00	0,00
Mg	0,33	0,31	0,39
Mn	0,03	0,03	0,04
Mo	0,00	0,00	0,00
Na	0,06	0,06	0,07
Nb	0,00	0,00	0,01
Nd	0,00	0,00	0,00
O	5,56	5,31	6,26
P	0,01	0,01	0,01
Pb	0,03	0,01	0,03
Pr	0,00	0,00	0,00
S	27,10	27,14	26,36
Si	2,75	2,63	3,03
Sm	0,00	0,00	0,00
Sn	0,16	0,19	0,30
Ta	0,00	0,00	0,01
Ti	0,01	0,02	0,02
Zn	43,86	43,23	41,28
Zr	0,00	0,00	0,00
Total	**99,99**	**99,99**	**100,00**

Appendix IV. Mineralogy Data

Table 21. Mineralogical composition of different feed samples by XRD

Mineral	Bulk	+50-80 µm	-50 µm
	Percentage, %		
Sphalerite	79,3	83.8	76.6
Arsenopyrite	5,8	4.9	5.4
Chalcopyrite	4.4	3.9	4.0
Pyrite	0.7	2.0	1.5
K-feldspar	5.1		
Quartz	4.7	3.8	4.8
Sulphur		1.6	1.4
Chlorite			1.7
Actinolite			4.5
Total	100	100	100

Table 22. Mineralogical compositions of the feed materials by MLA

Mineral	Bulk	+50 -80 µm	-50 µm
	Percentage, %		
Sphalerite	77,88	77,09	73,84
Chalcopyrite	2,92	3,34	3,57
Arsenopyrite	2,86	3,64	3,84
Garnet	2,85	2,68	3,01
Amphibole	2,40	2,23	3,24
Quartz	2,22	2,17	2,17
Pyrite	2,19	2,22	2,48
Mica	1,53	1,46	1,60
Iron oxide	1,37	1,30	1,53
Feldspar	1,05	1,03	1,32
Chlorite	1,01	0,90	1,13
Other minerals	1,73	1,94	2,26
Total	**100,00**	**100,00**	**100,00**

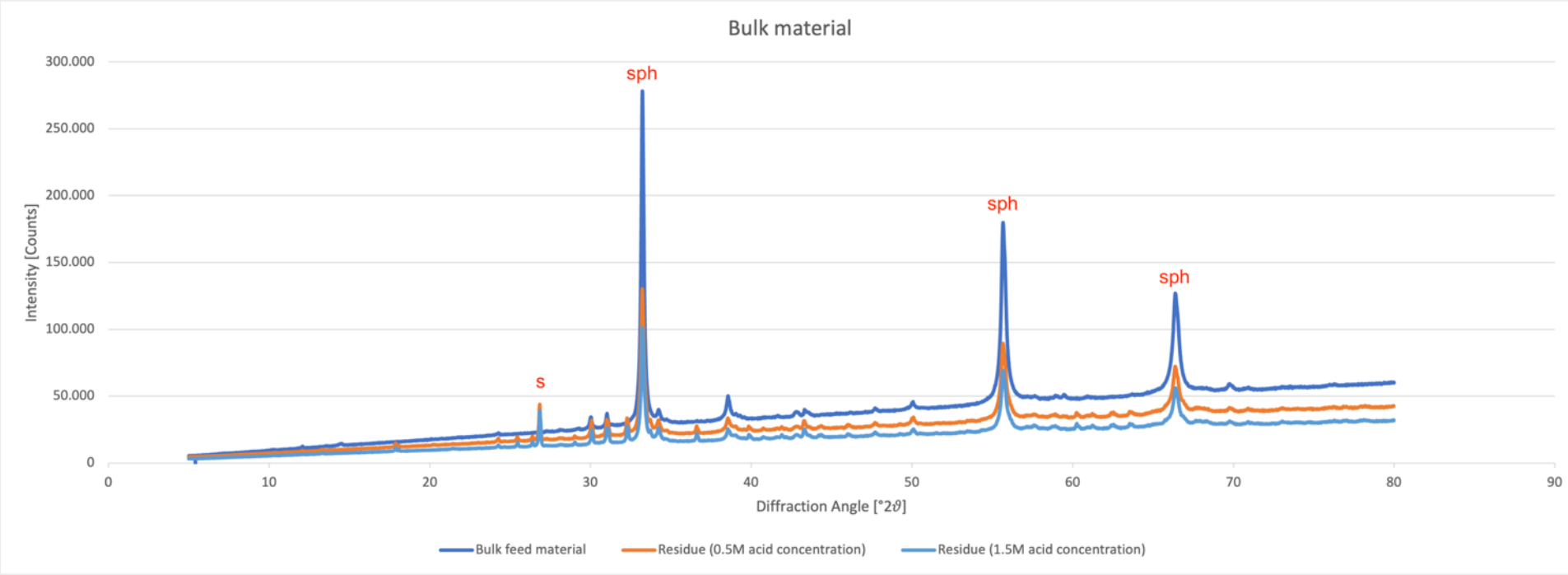

Figure 27. Comparison of XRD diffractogram of bulk feed material and residues from different acidic conditions

Appendix V. Digital Appendix (CD)

Folder 1 Master_Thesis_Shineod_Mongoljiibuu.docx

Folder 2 MLA data.xslx